# Filme nanostructurate functionale obtinute prin metoda arcului termoionic in vid

**C. P. Lungu[1], I. Jepu[1], C. Porosnicu[1], A. Anghel[1], A.M.Lungu[1], P. Chiru[1], C.Ticos[1], I. Mustata[1], V. Kuncser[2], V. Ionescu[3], V. Ciupina[3], M. Osiac[4], G.E. Iacobescu[4]**

*[1]INCD pentru Fizica Laserilor, Plasmei si Radiatiei,*

*[2]INCD pentru Fizica Materialelor,*

*[3]Universitatea "Ovidius" din Constanta,*

*[4]Facultatea de Fizica, Universitatea Craiova din Craiova*

# CUPRINS

- **Metoda Arcului Termoionic in Vid (TVA);**
- **Filme GMR/TMR multistrat ;**
- **Filme tribologice**
- **Filme pentru tehnologii nucleare**

# Principiul metodei arcului termoionic in vid (TVA)

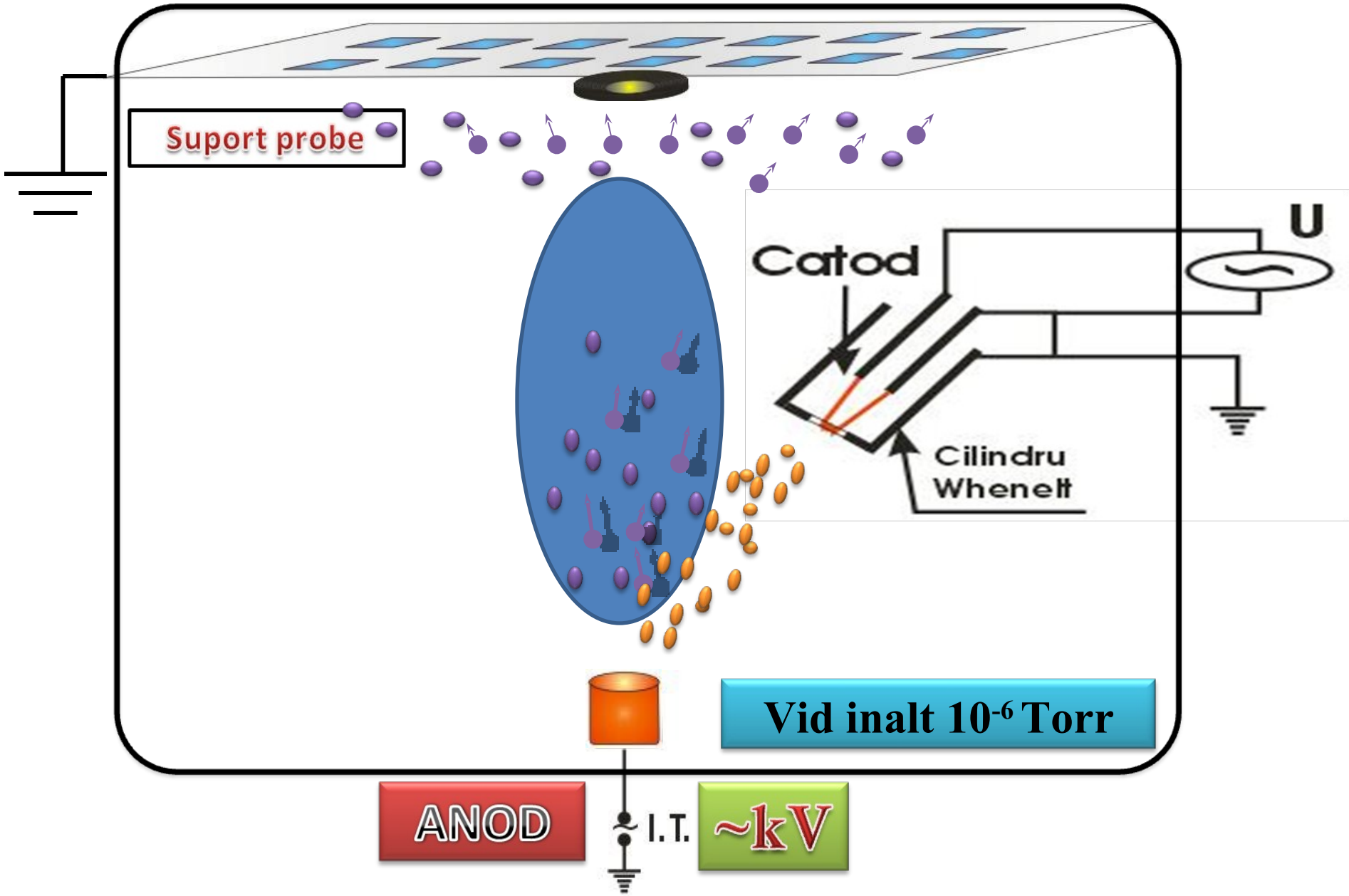

# Aprinderea plasmei TVA

# SIMETRIE CILINDRICA TVA

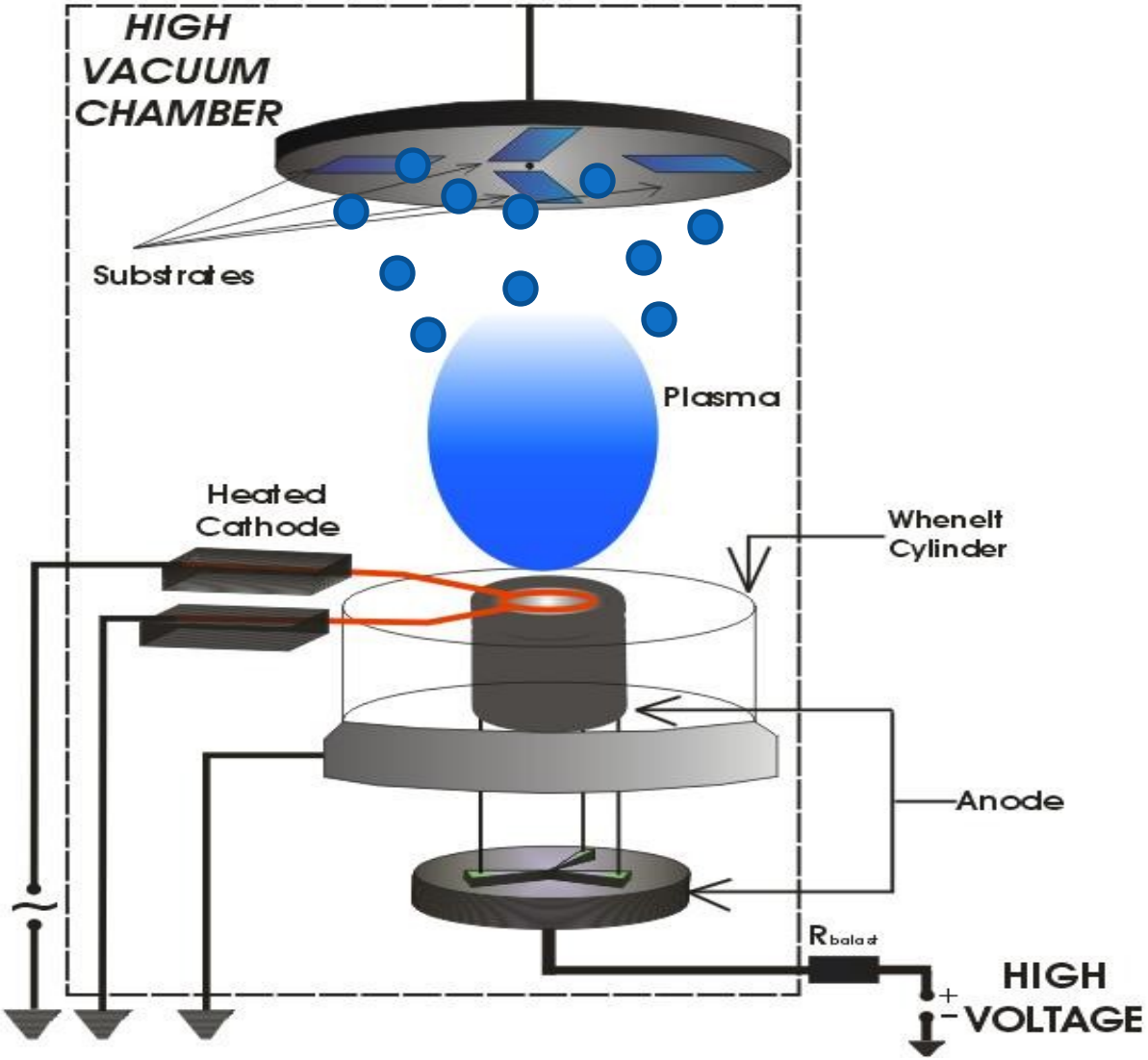

# FORMA PLASMEI SI CONTROLUL ENERGETIC AL IONILOR

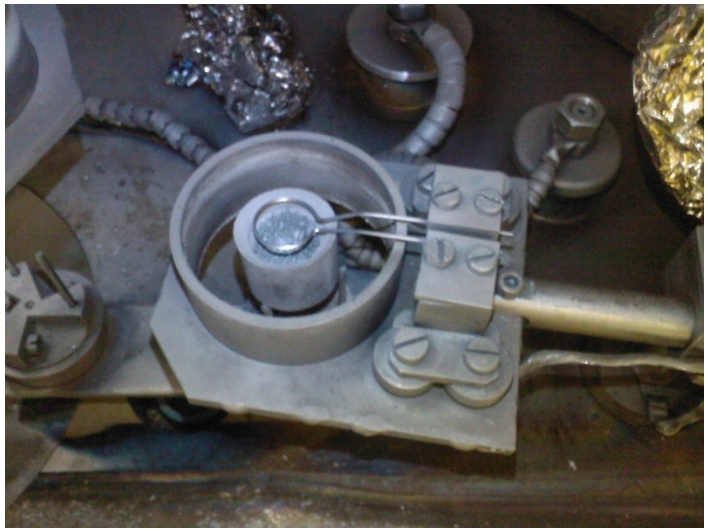

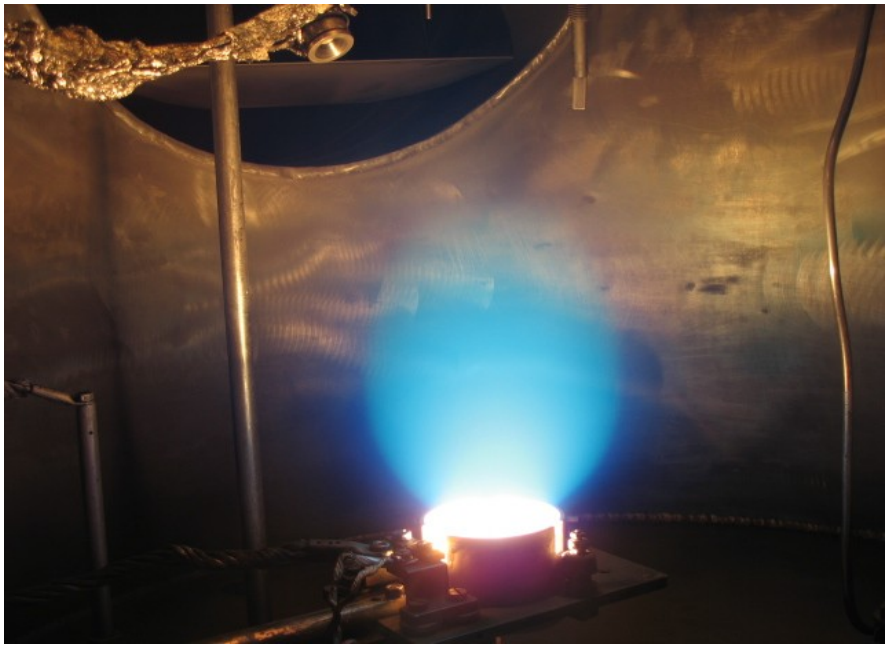

ℙ= 1550W

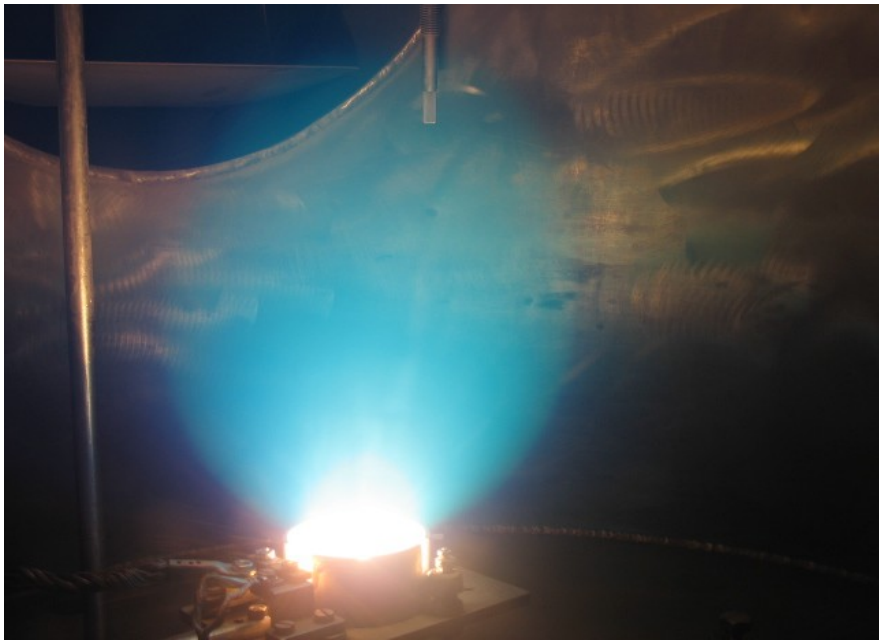

ℙ= 1800W

# Optimizarea parametrilor plasmei TVA

Caracteristicile I-V ale unei plasme TVA in vapori de Ag si Cu, pentru diferite distante intre anod si catod, curentul pe filament fiind constant

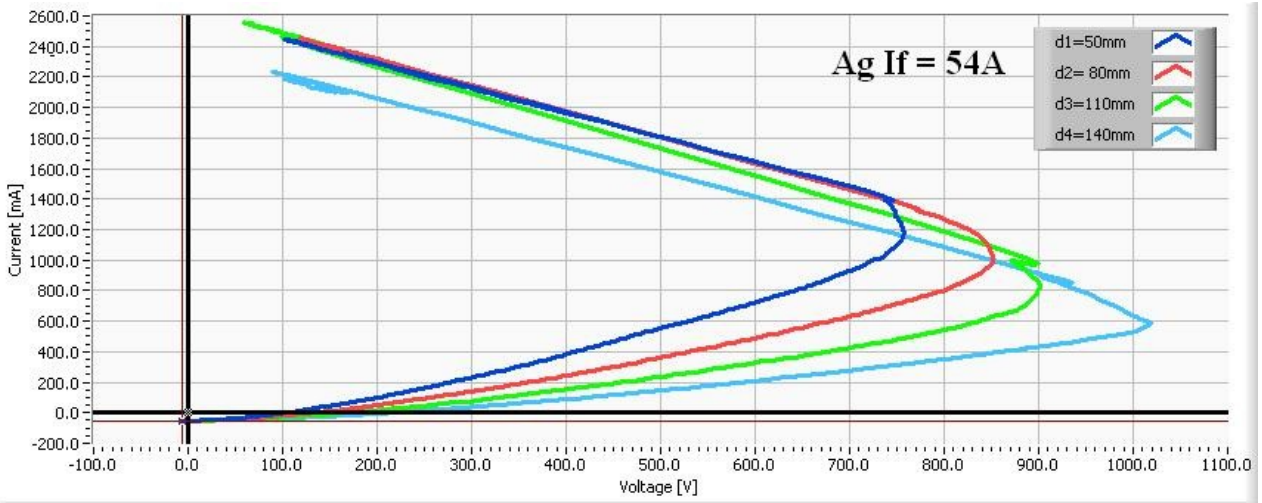


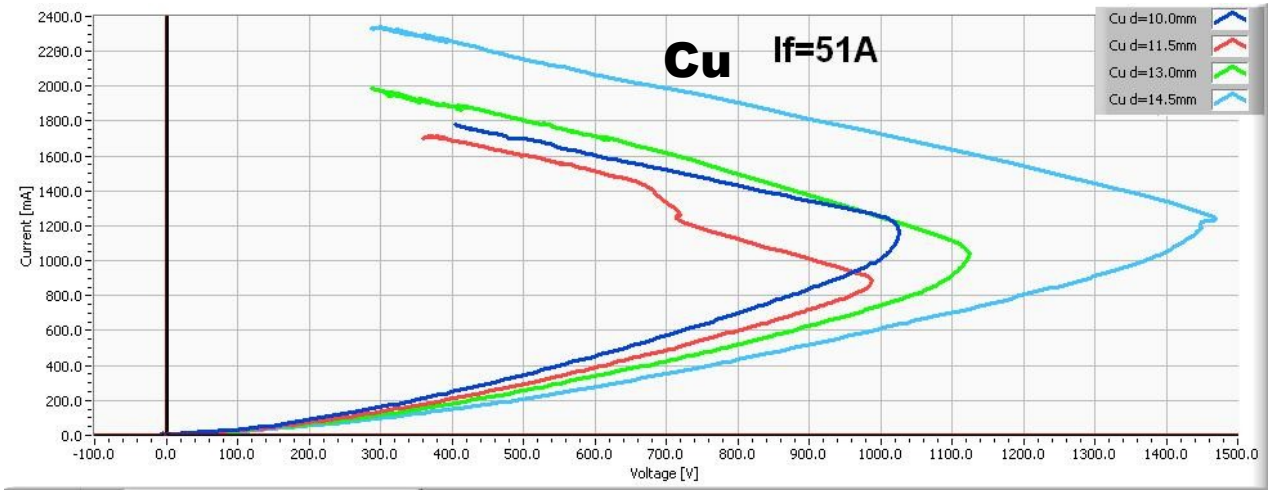

# Optimizarea parametrilor plasmei TVA

Caracteristicile I-V ale plasmei TVA in vapori de Ag si Cu pentru diferiti curenti de filament, distanta anod catod fiind constanta

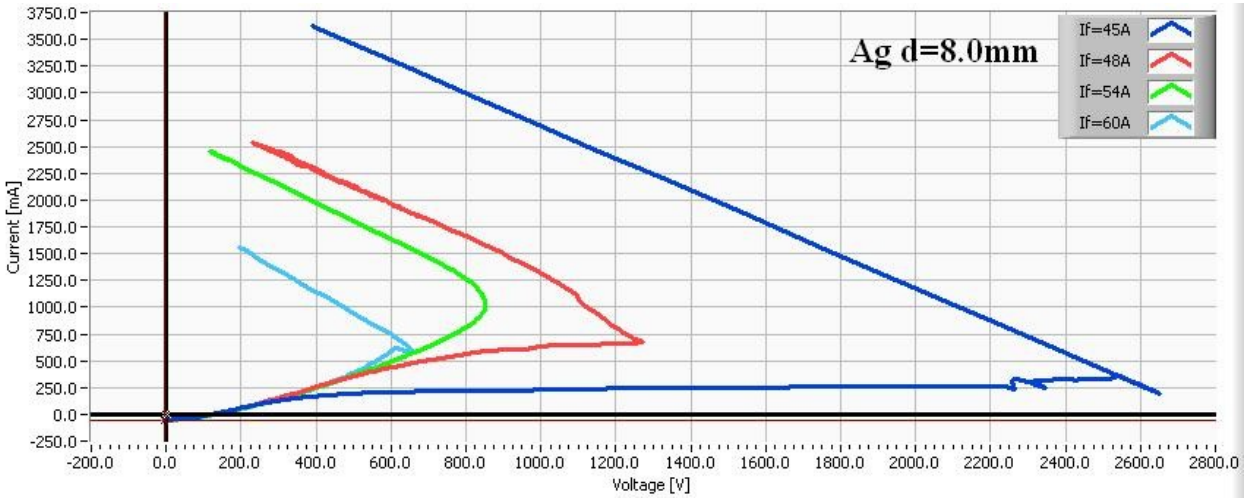


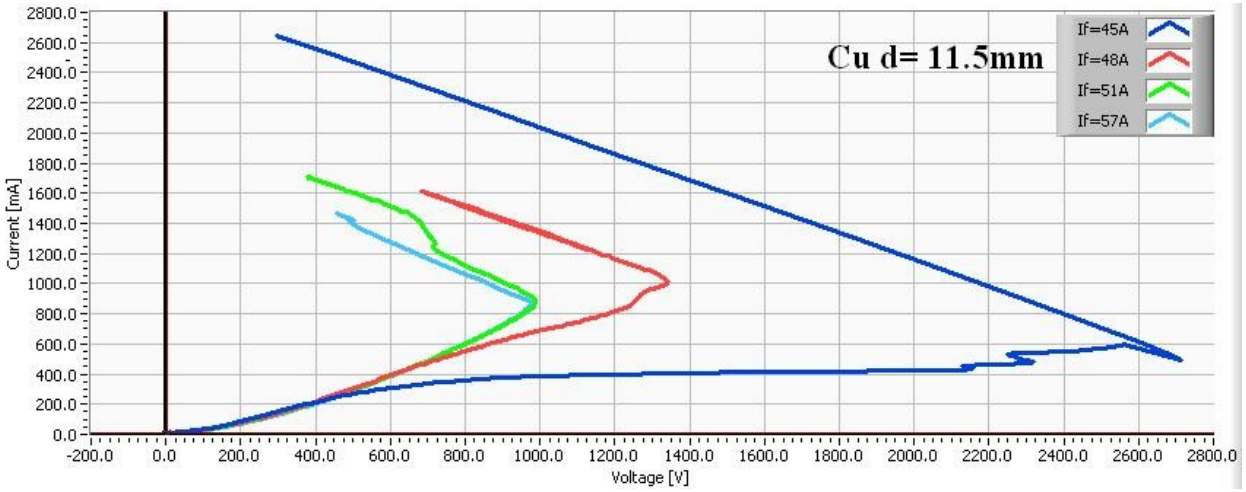

# PRINCIPALELE AVANTAJE ALE METODEI TVA

- **Puritatea ridicata a straturilor (datorita vidului inalt in care se efectueaza depunerea)**
- **Filmele cresc din plasma creată in vaporii puri ai materialului depus;**
- **Filmele sunt bombardate continuu de ioni energetici de aceeasi natura cu cei ai filmului depus;**
- **Energia ionilor poate fi controlata prin reglarea temperaturii catodului si tensiunea anod - catod**

# Depuneri Multistrat

# Sistemul Anodic pentru depunerea multistrat

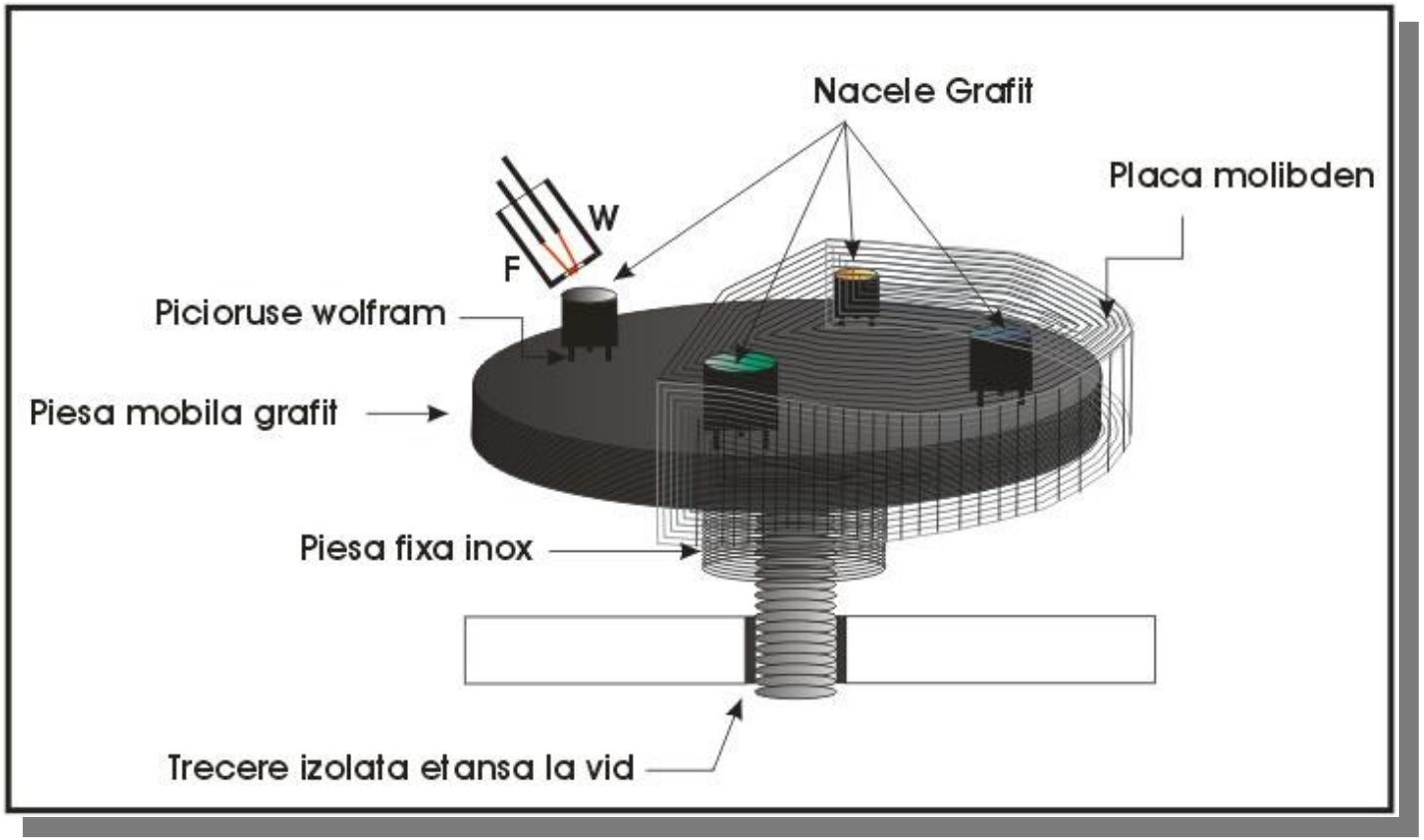

# Schema montajului

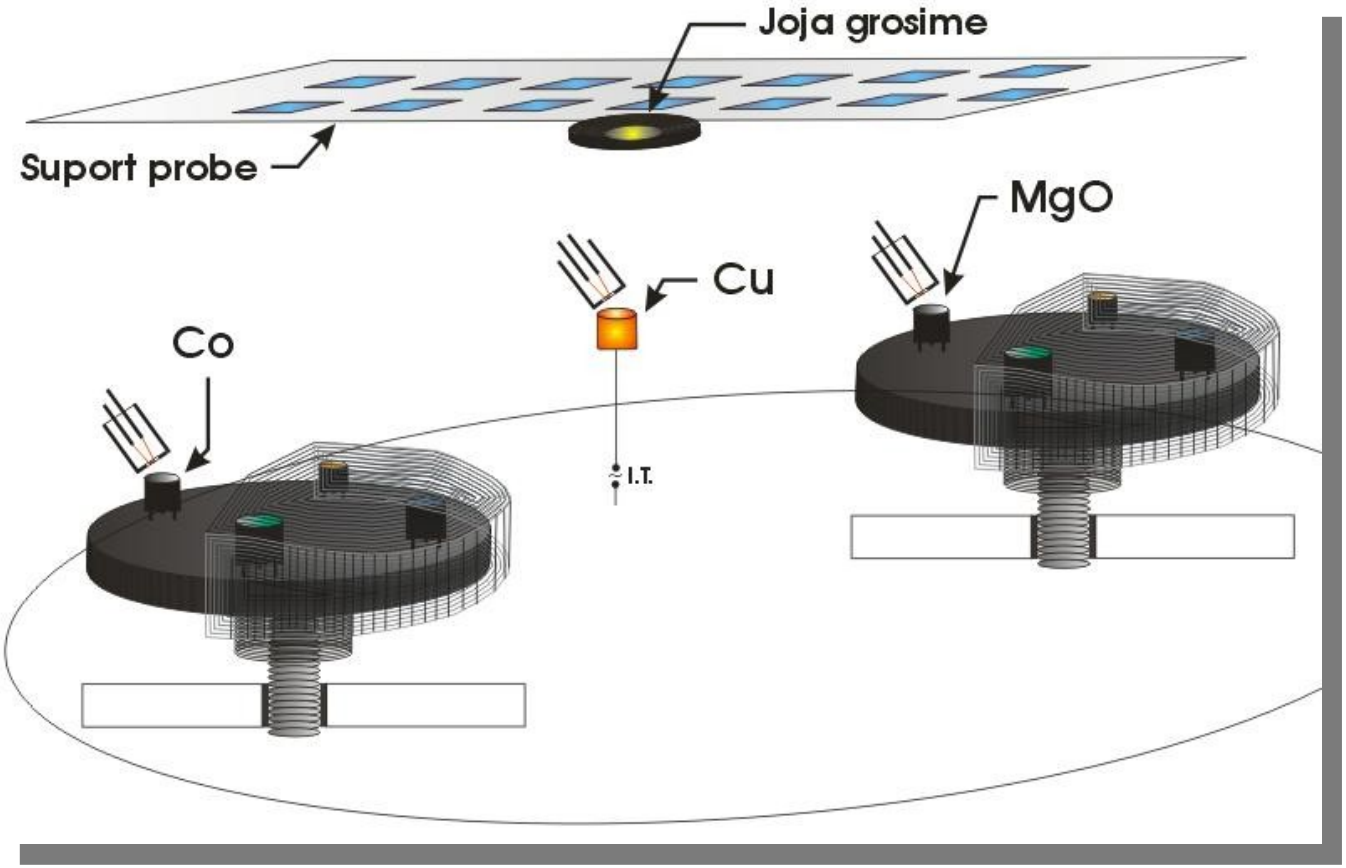

# Depuneri Multistrat

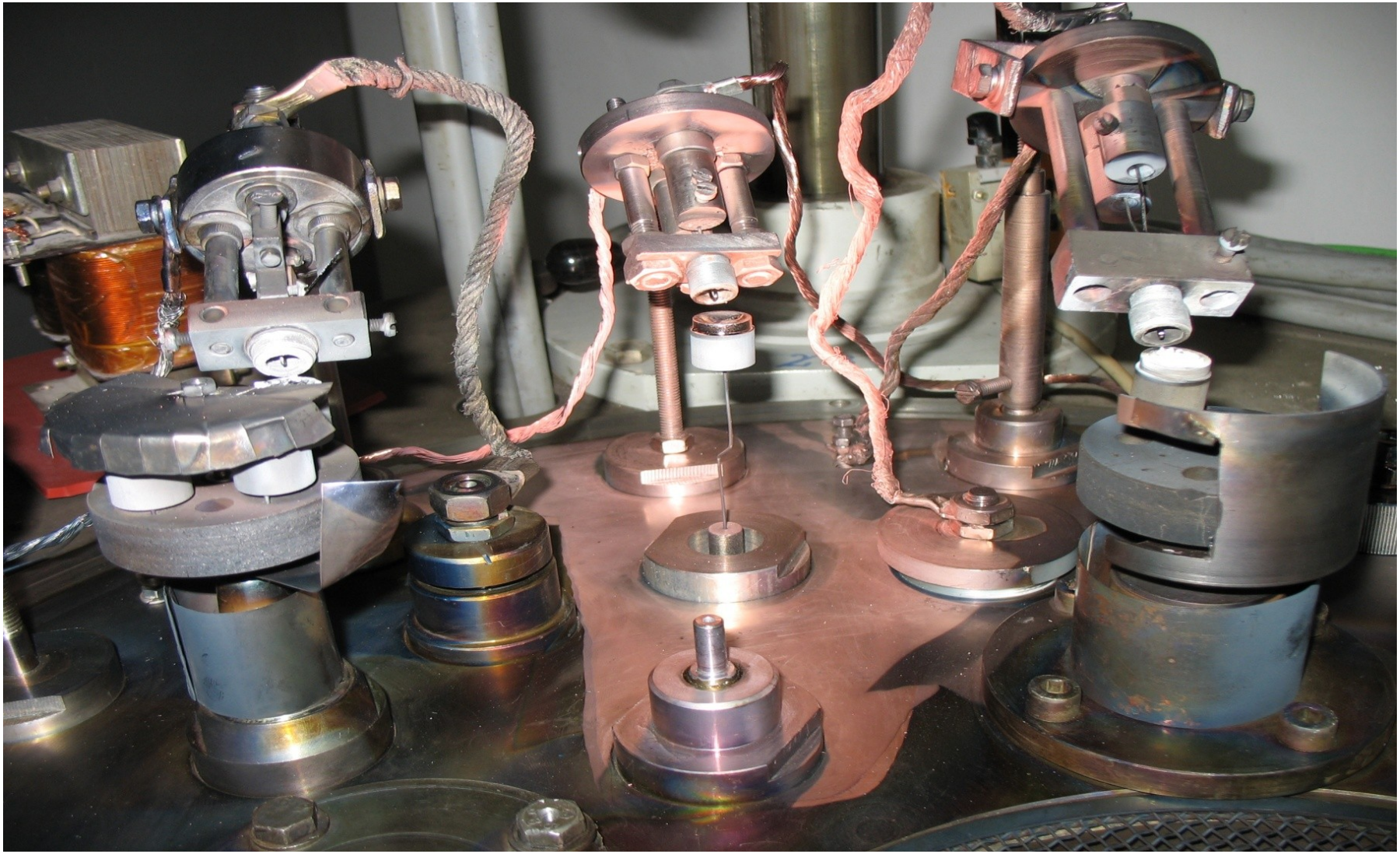

# Depuneri Multistrat

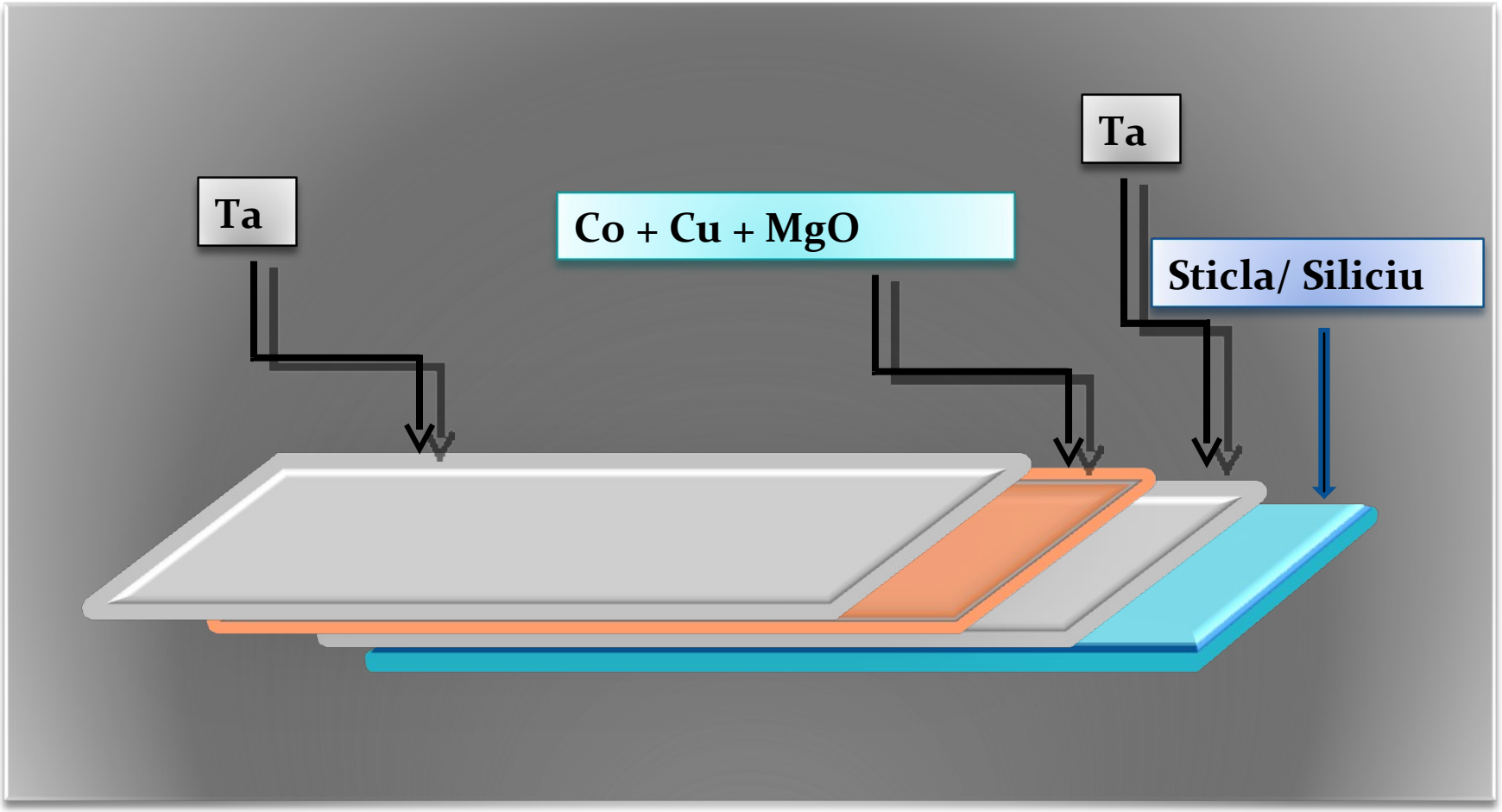

# Depuneri Multistrat

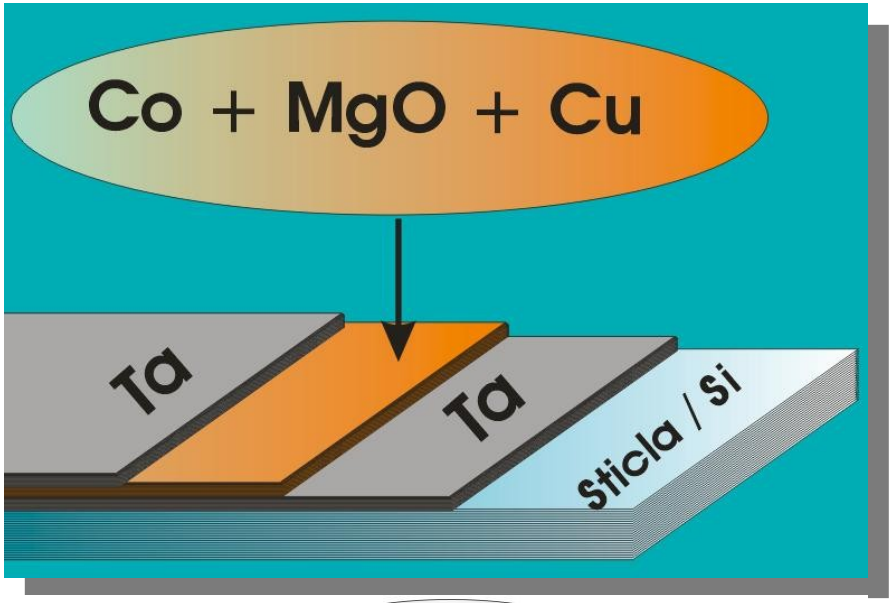


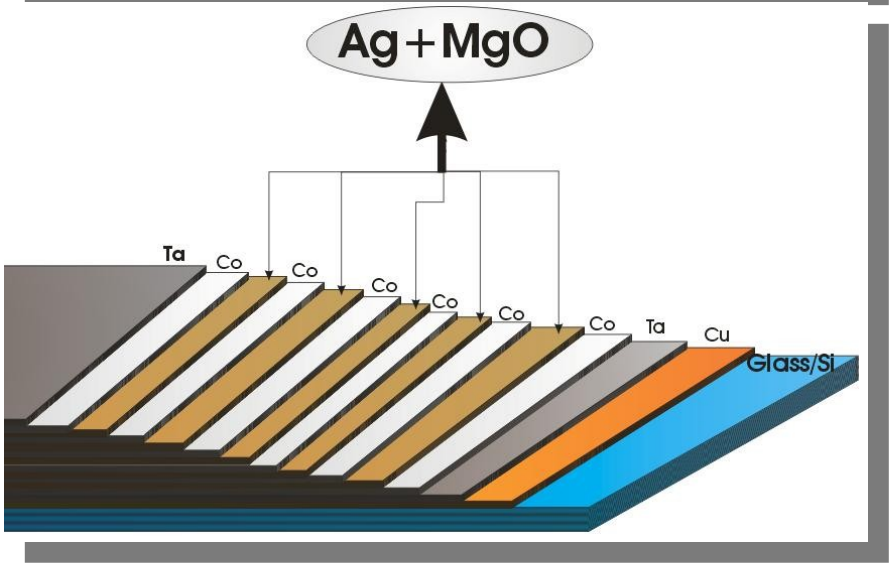

# Analizele SEM ale filmelor multistrat

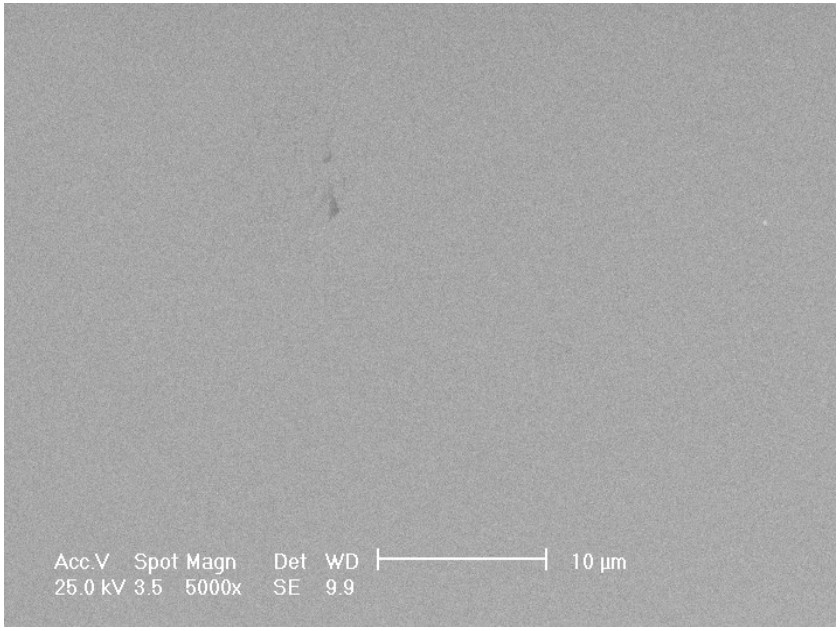


Proba 2.10
Co/MgO/Cu

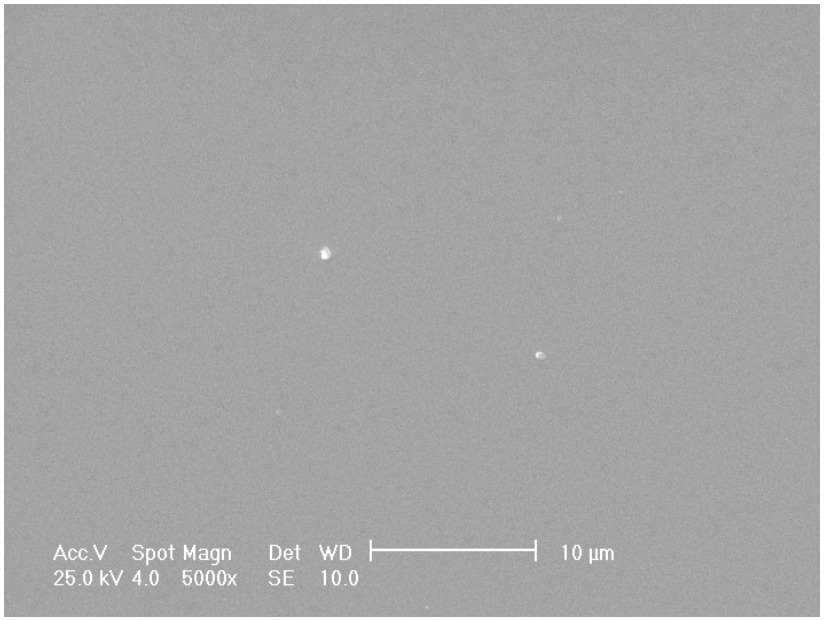


Proba 2.6
Co/MgO/Cu

# Concentratiile masice ale fiecarui material in parte

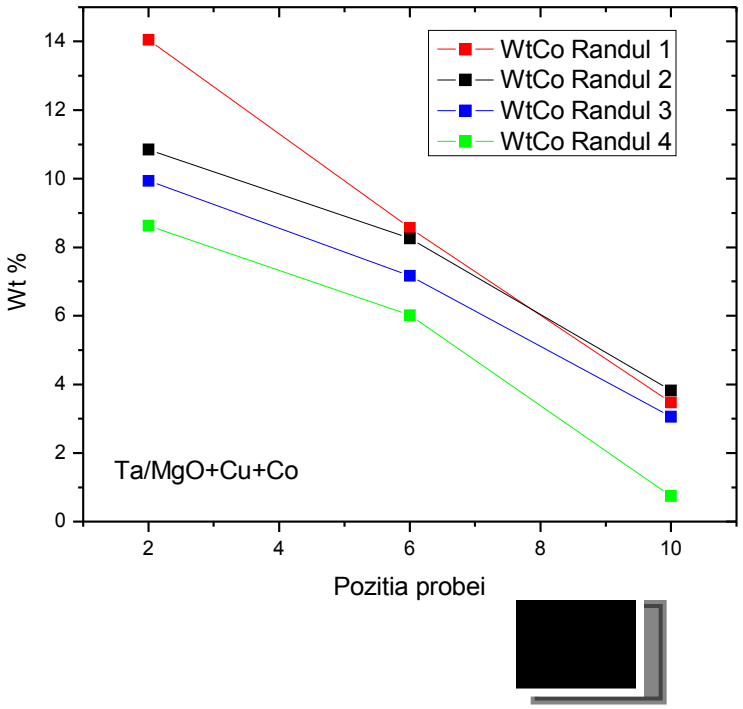


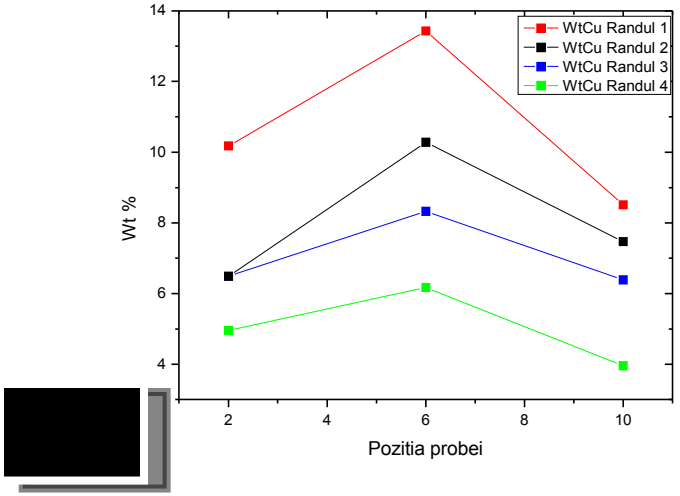


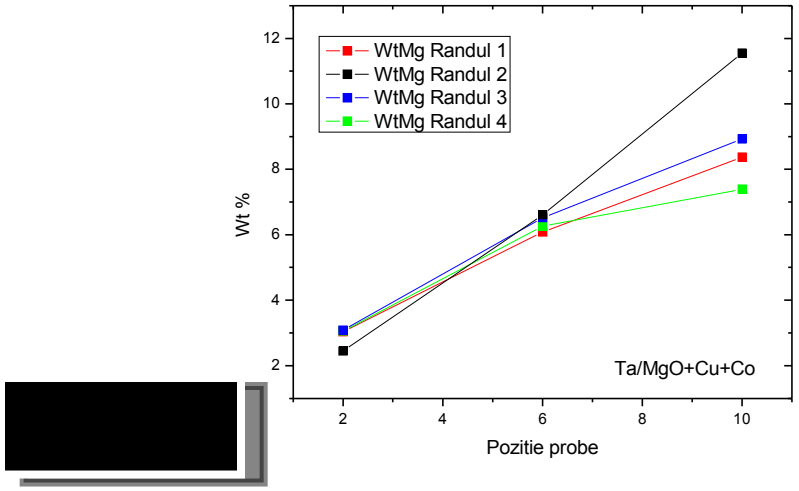

# Schema contactelor masuratorii in patru puncte

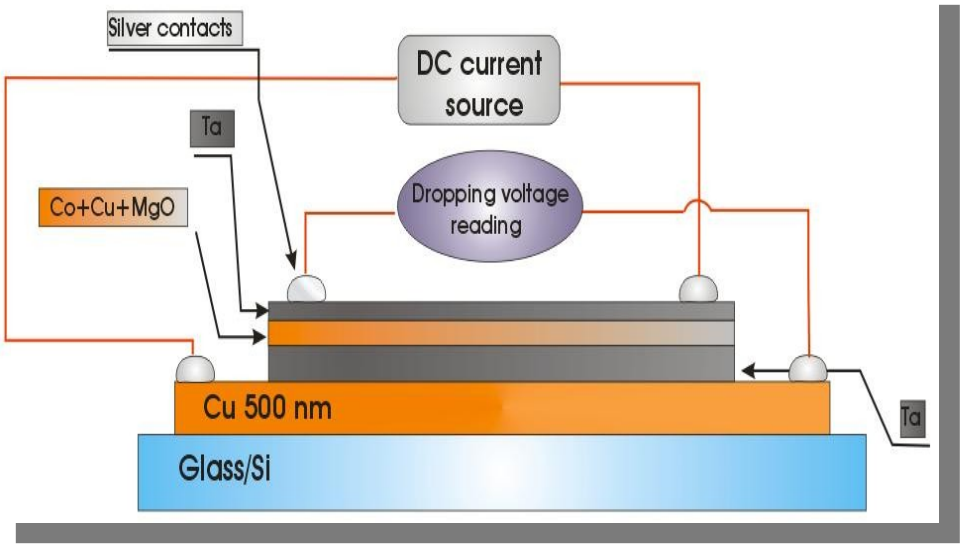


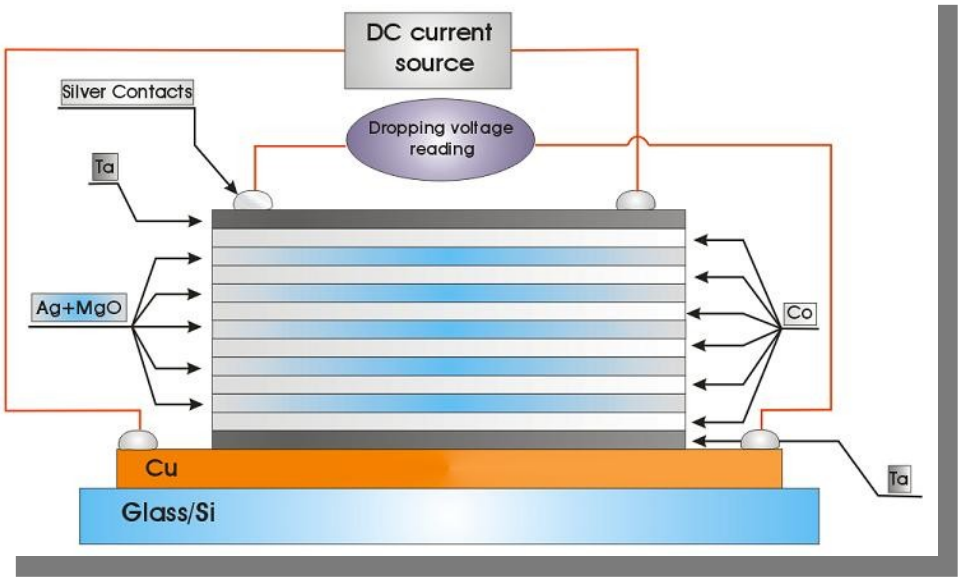

# Masuratori electrice efectuate pe probele multistrat

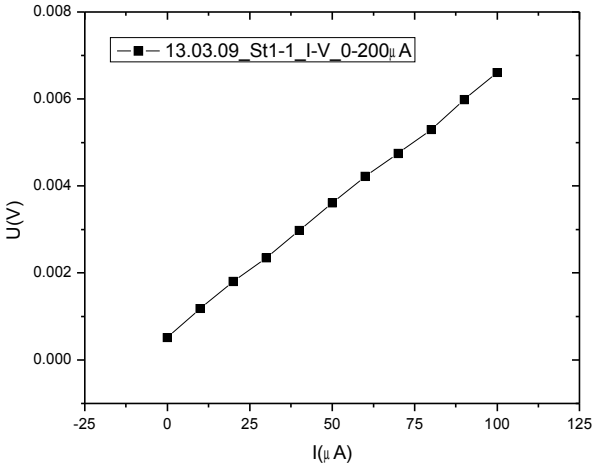


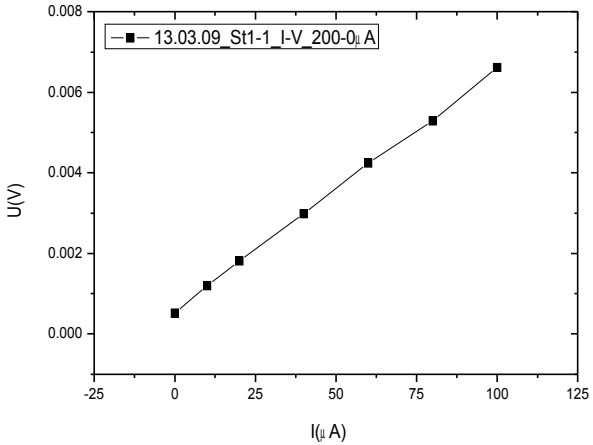


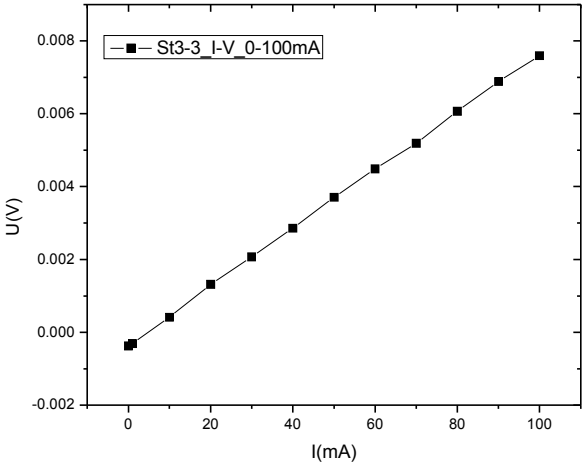


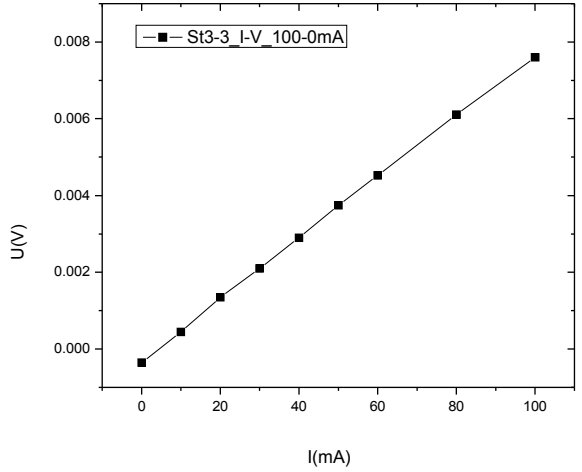

# Masuratori MOKE efectuate pe probele multistrat

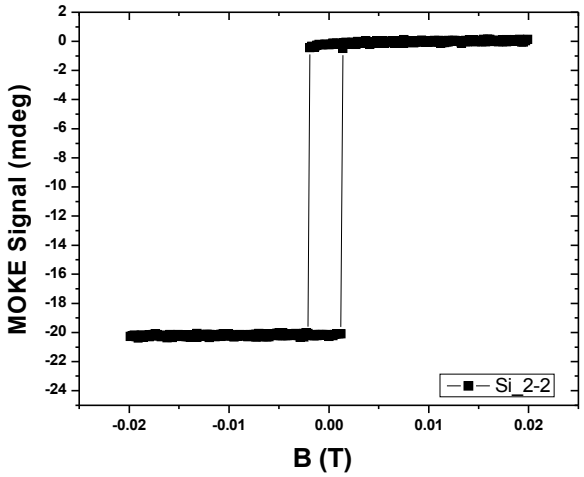


**Concentratie mare de Co**

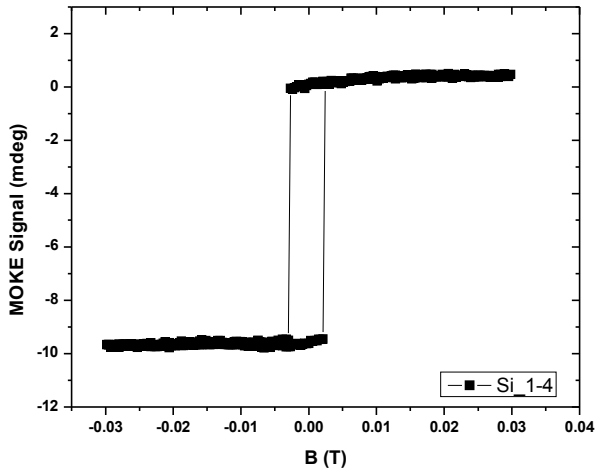


**Concentratie mare de Cu**

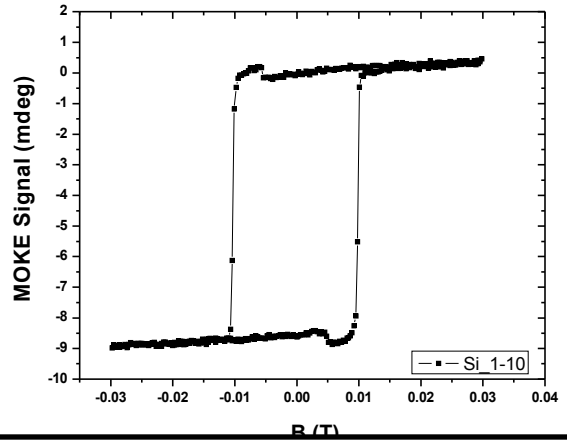


**Concentratie mare de MgO**

# Masuratori MR pe probele multistrat

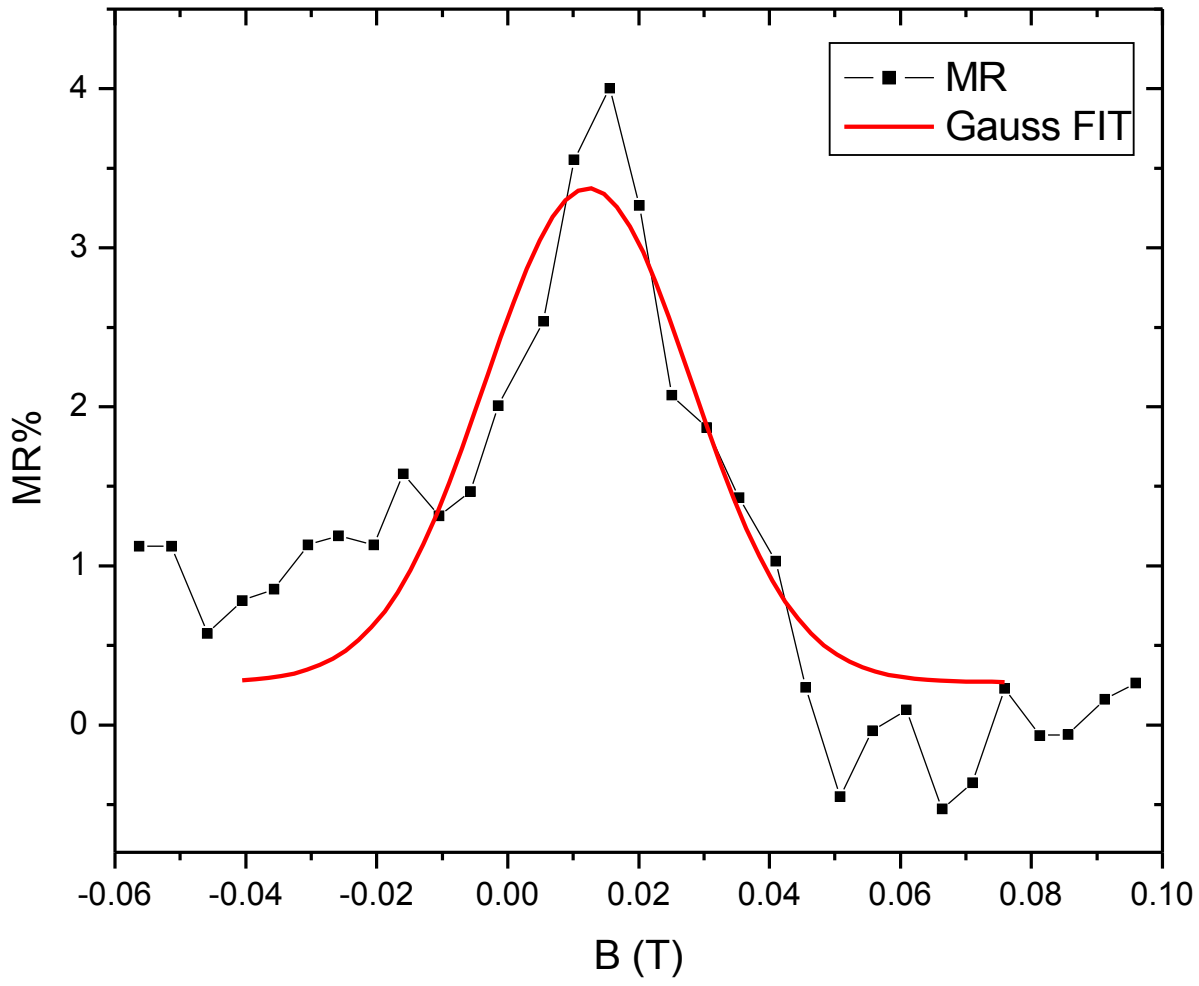


Proba 2.3

# Masuratori MR pe probe multistrat

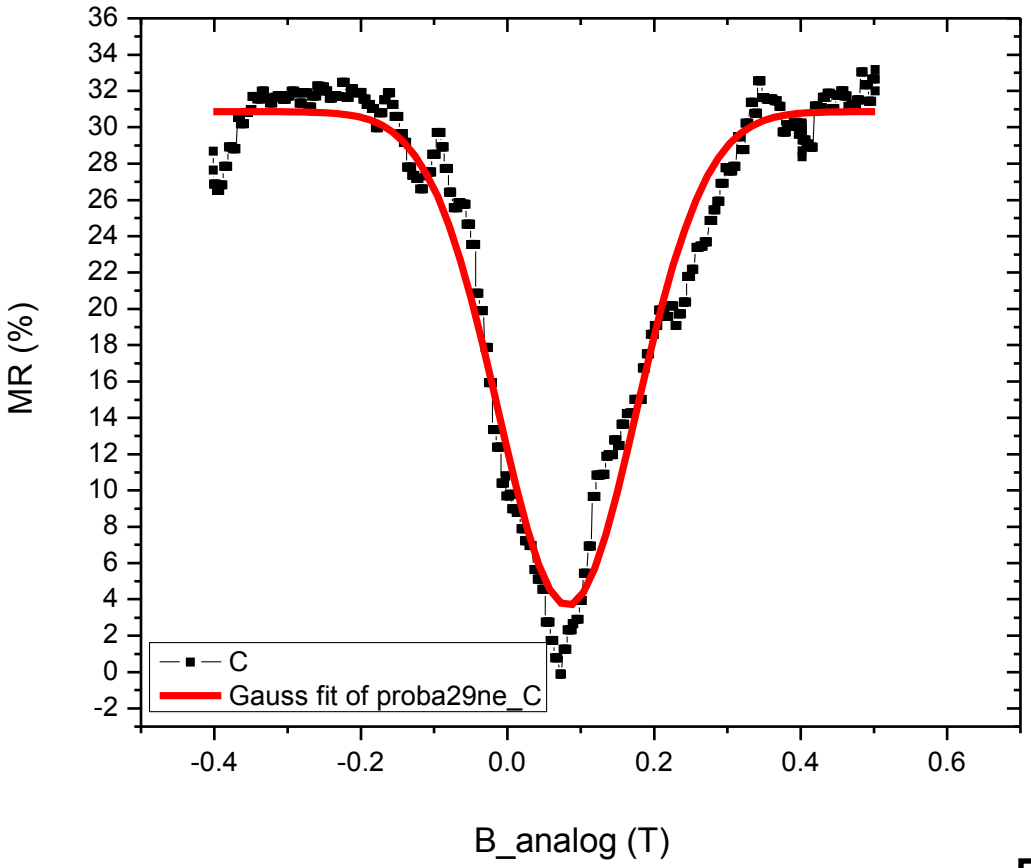


Proba 2.9

# FILME GRANULARE MAGNETOREZISTIVES

# Microscopie de forta magnetica (MFM):

# filme Fe-Cu

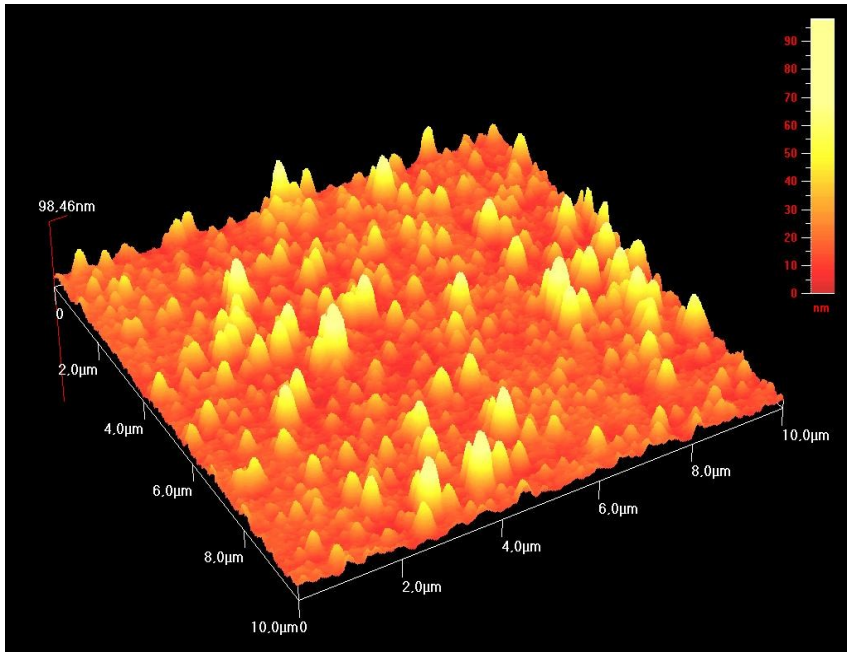


Topographic AFM image of a Fe-Cu film (B)

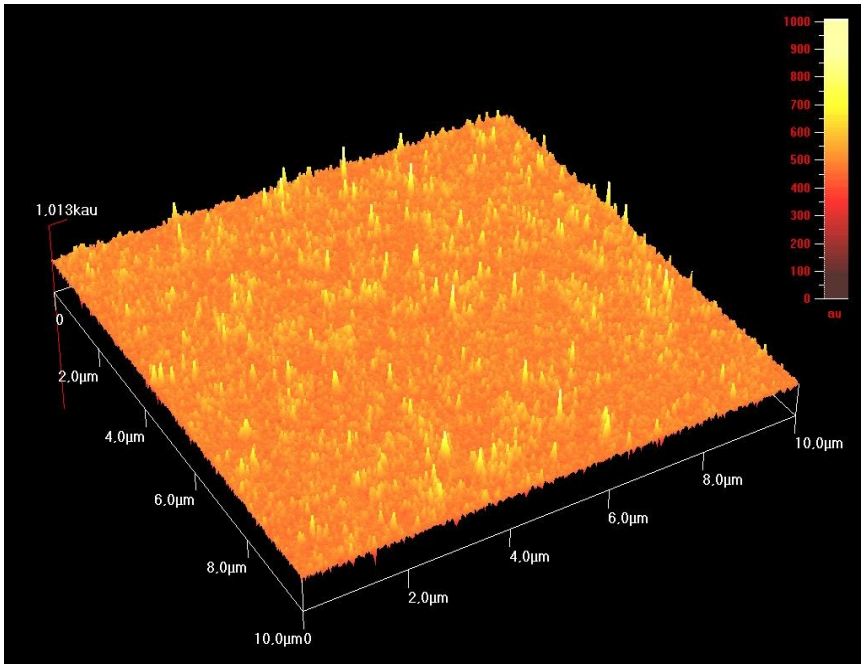


Magnetic domain distribution in a Fe-Cu film (B)

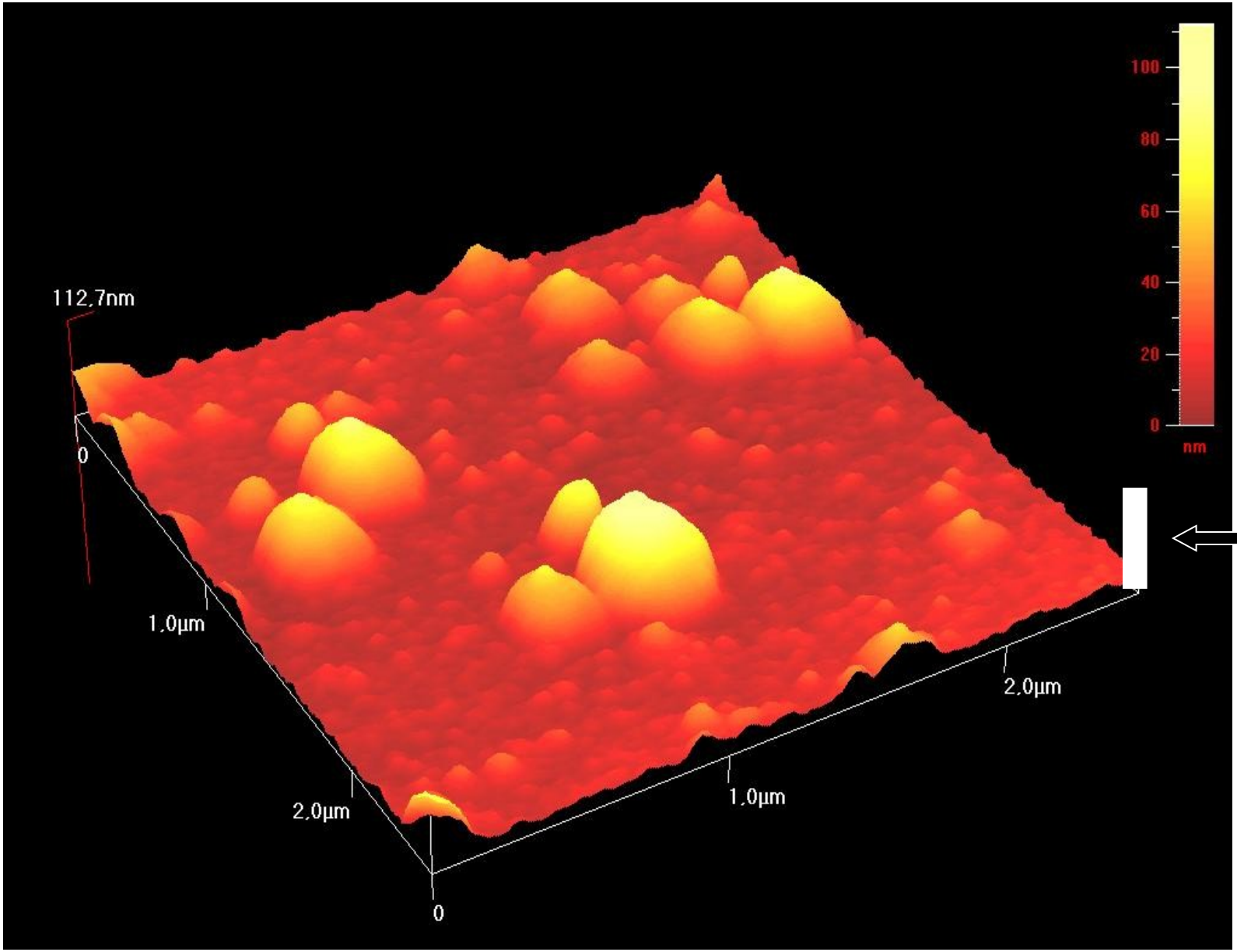


Topographic MFM image

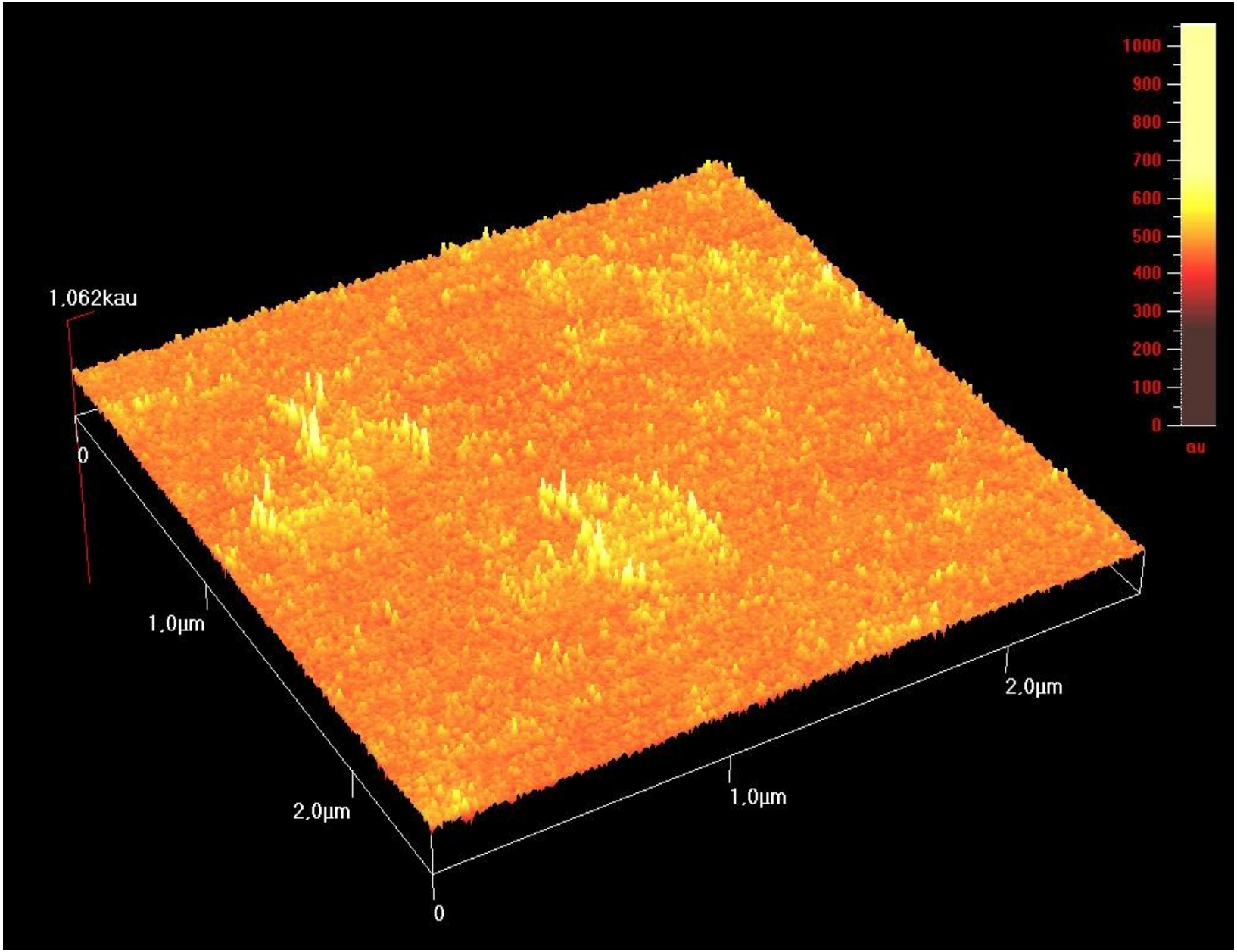


Magnetic domains distribution of a Fe-Cu film

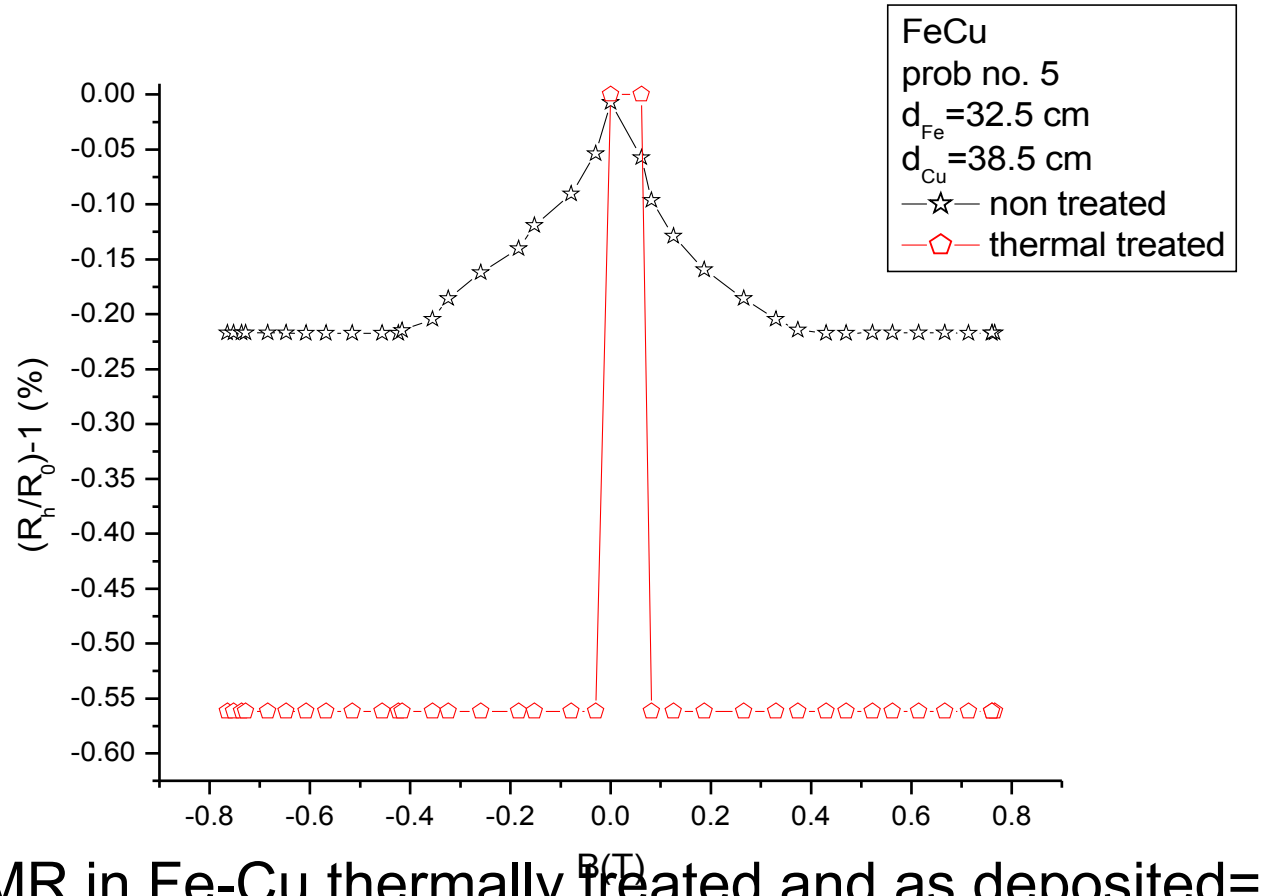


GMR in Fe-Cu thermally treated and as deposited= high abrupt variation=uniform dimensional distribution of formed domains

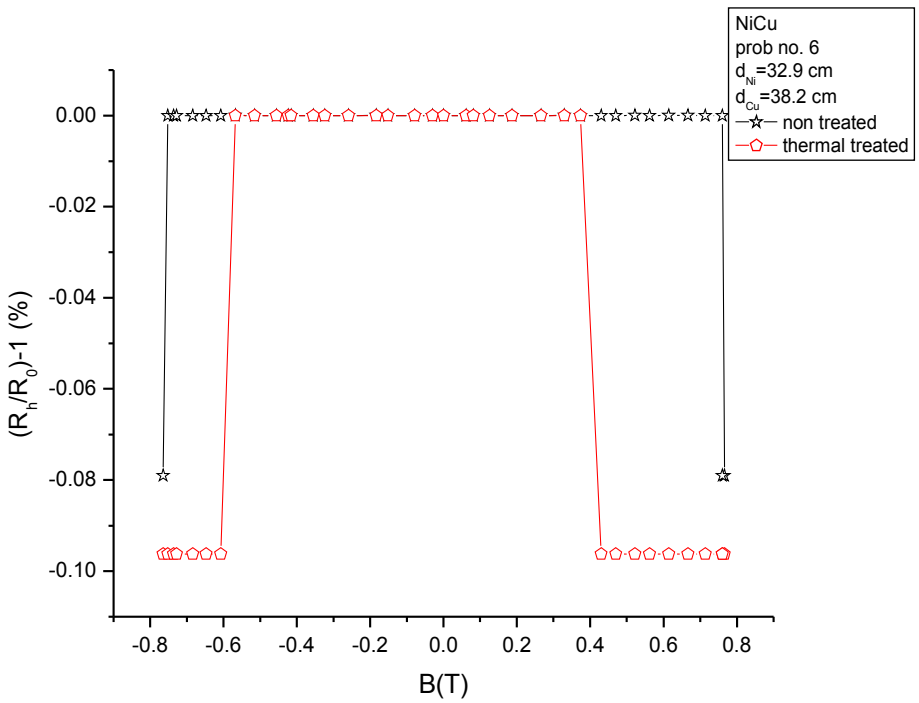


# GMR in Ni-Cu composite layer

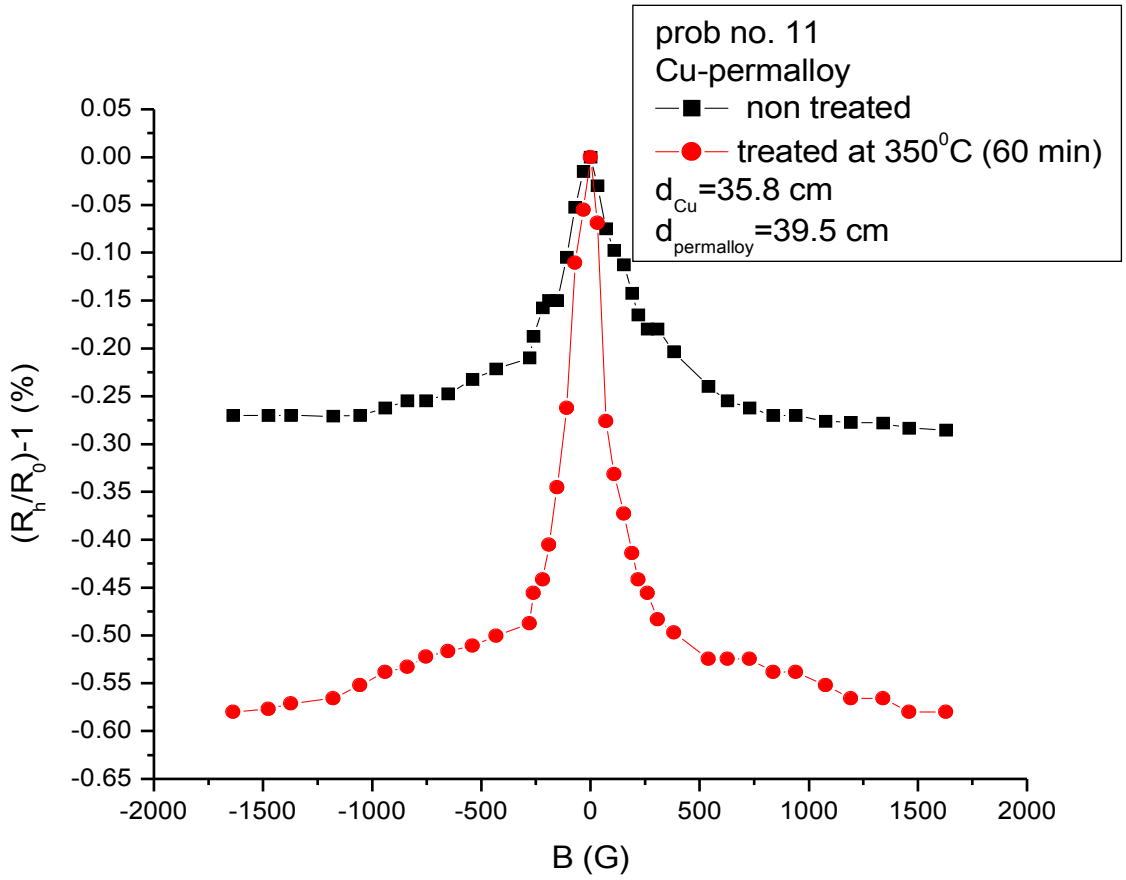


GMR in Cu-permalloy

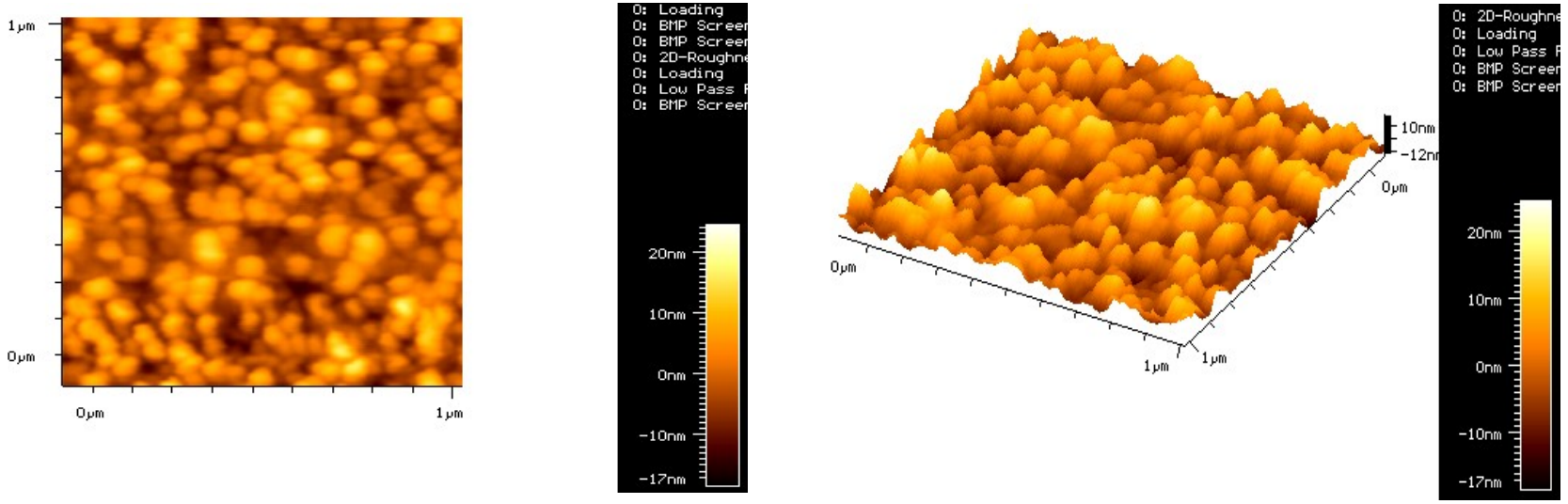


AFM images of the Co-Cu films

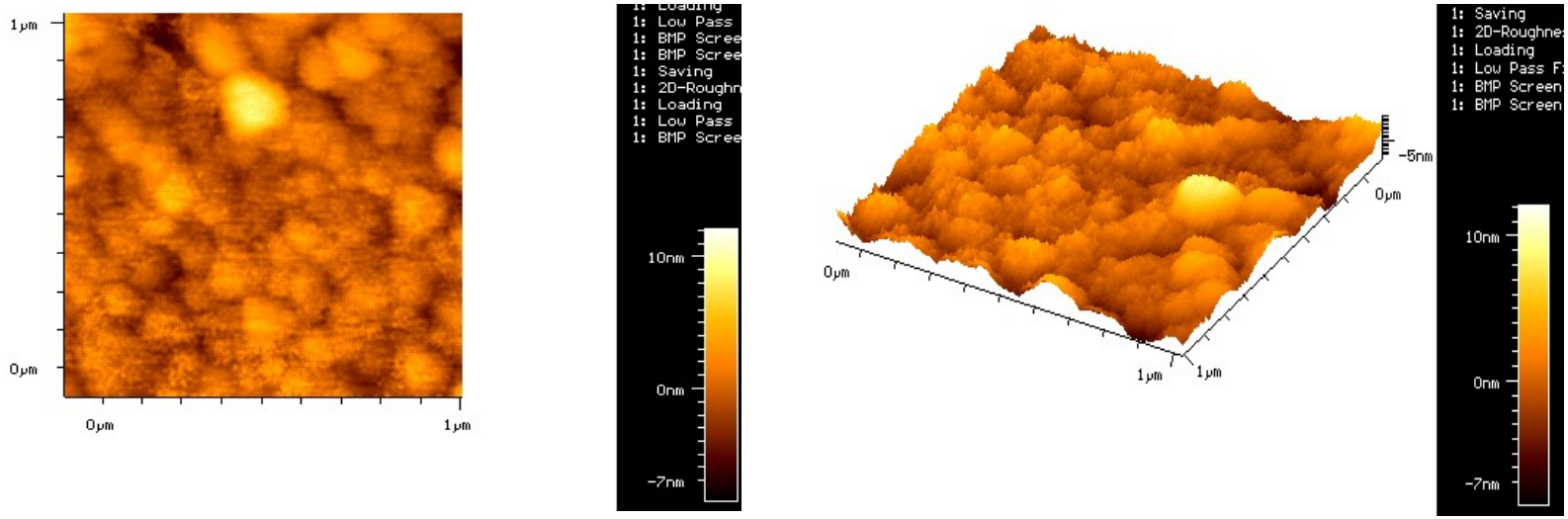


AFM images of the Fe-Cu films

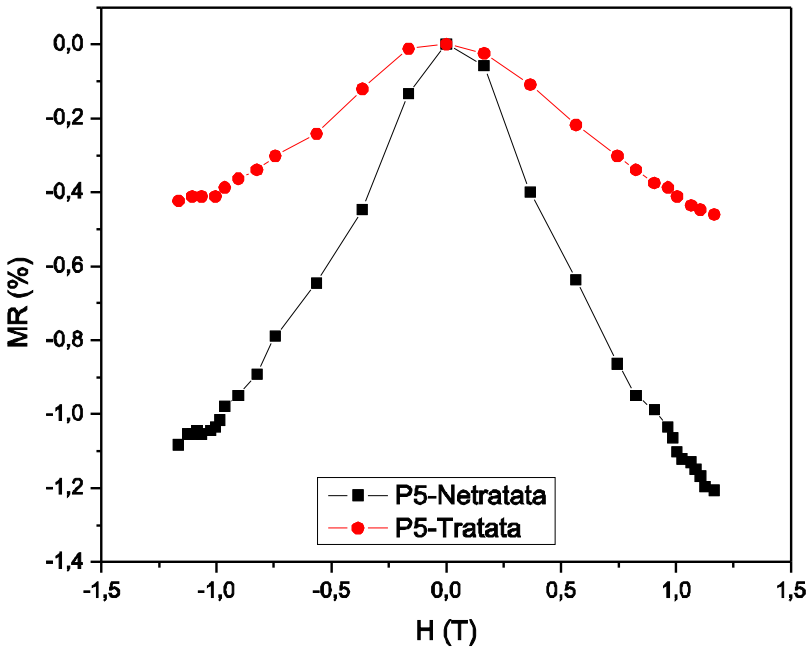


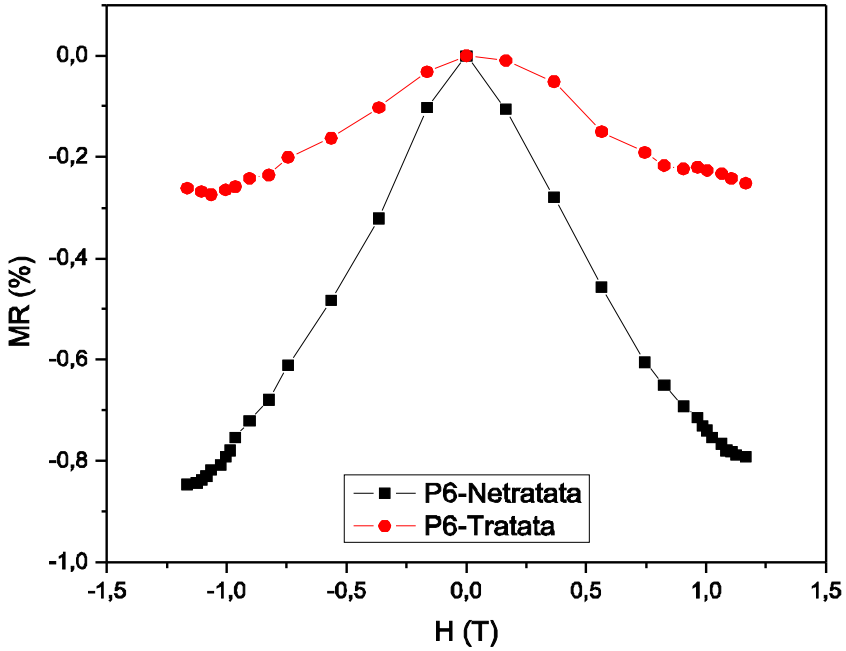


Magnetoresistance vs. applied magnetic field:
- As deposited (black line)
- Thermally treated (red line)

The decrease of the TMR effect after the thermal treatment is caused by:

-Strong oxidation of magnetic grains
-Partial percolation

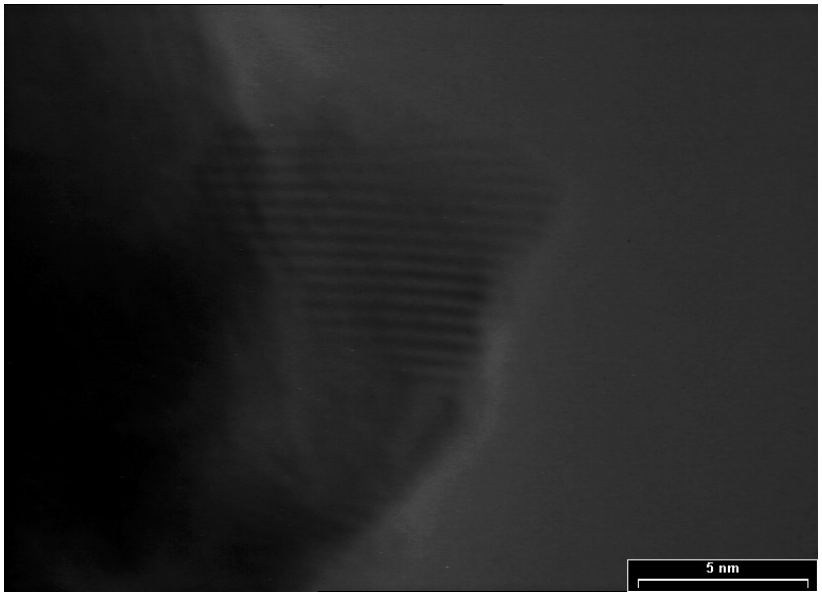


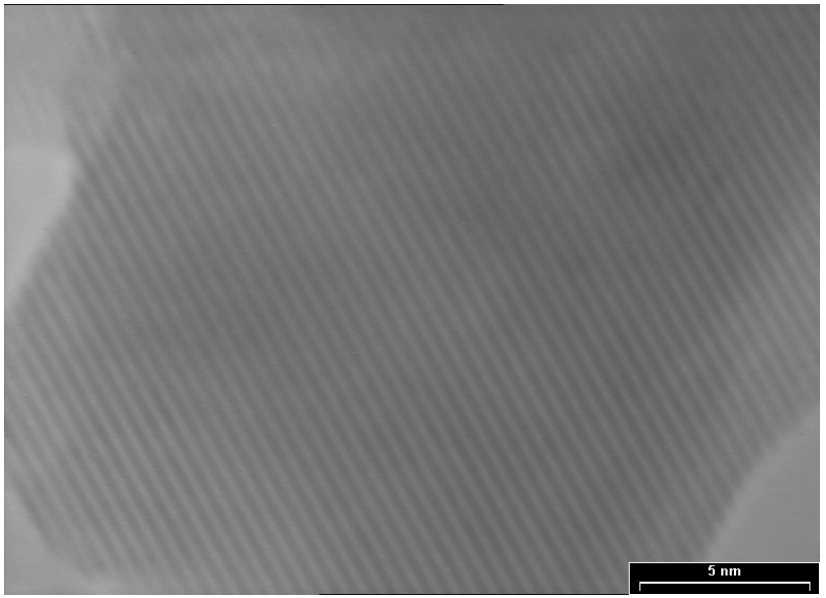


a) b)

HRTEM images on Co – MgO granular TMR films:
b) As deposited
c) Thermally treated

Observation: formation of large crystalline magnetic domains during the thermal treatment

# Filme compozite

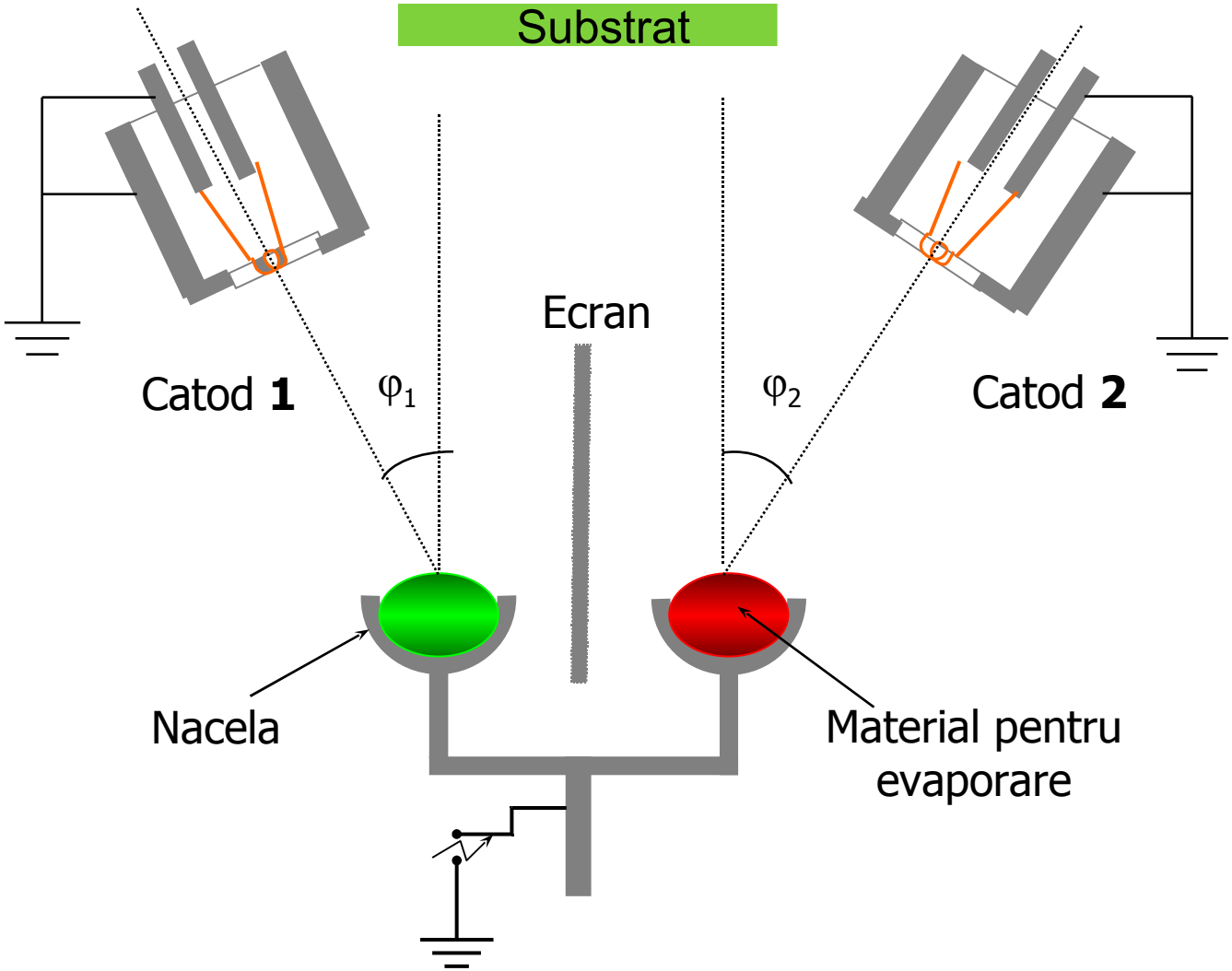

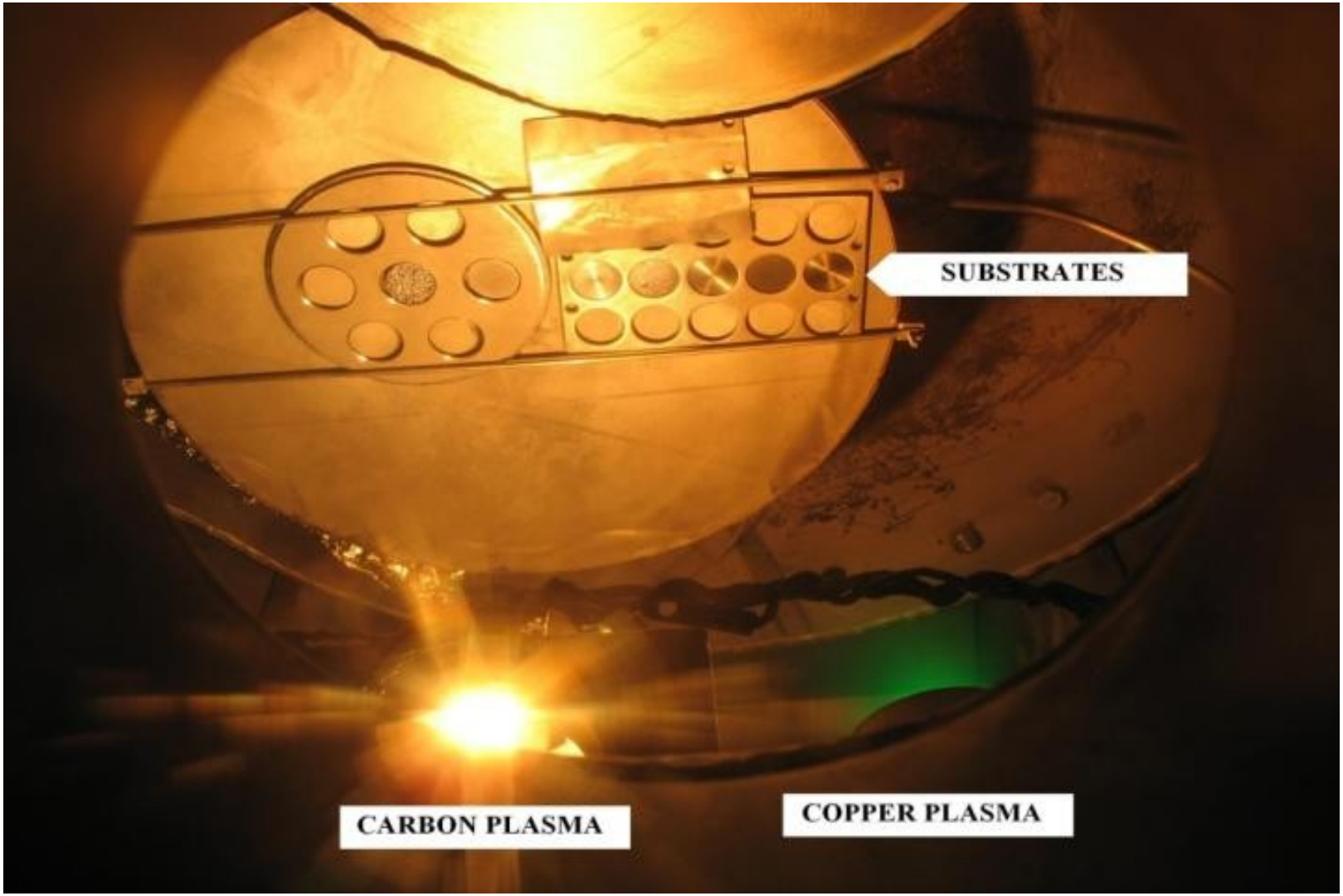
SUBSTRATES
CARBON PLASMA
COPPER PLASMA

# TVA Plasma Symmetry

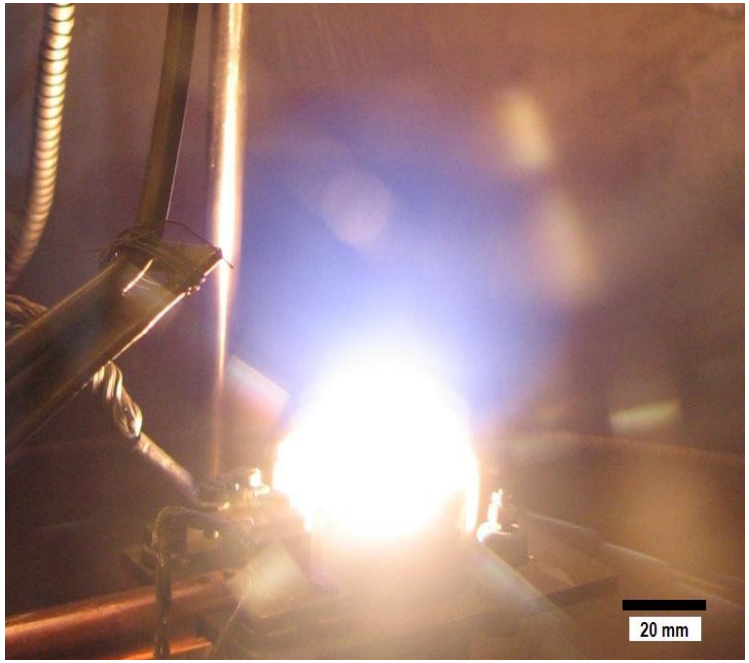


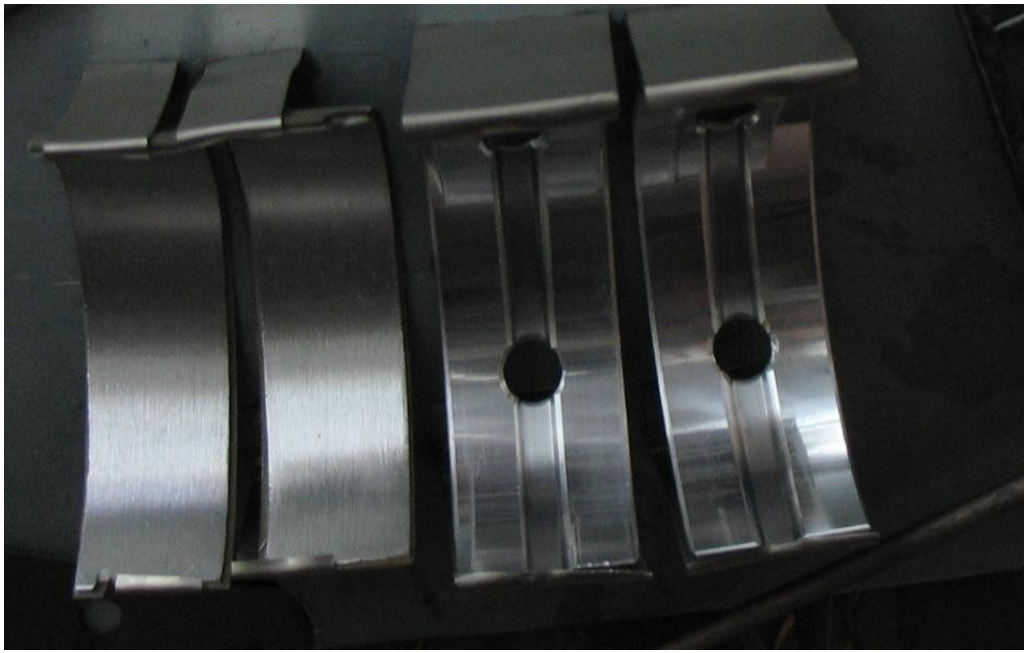

Wear scar on C-W film

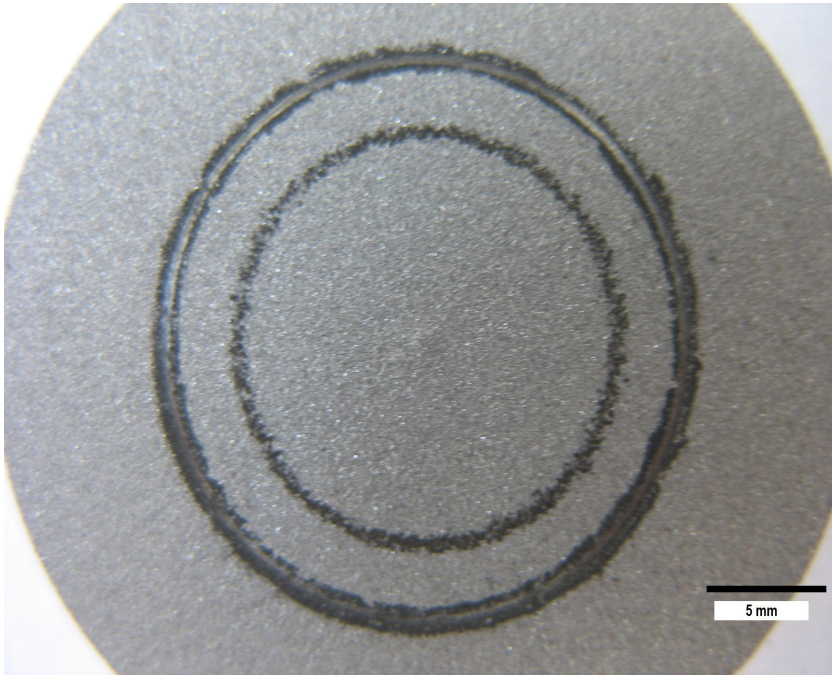


AFM of the wear track

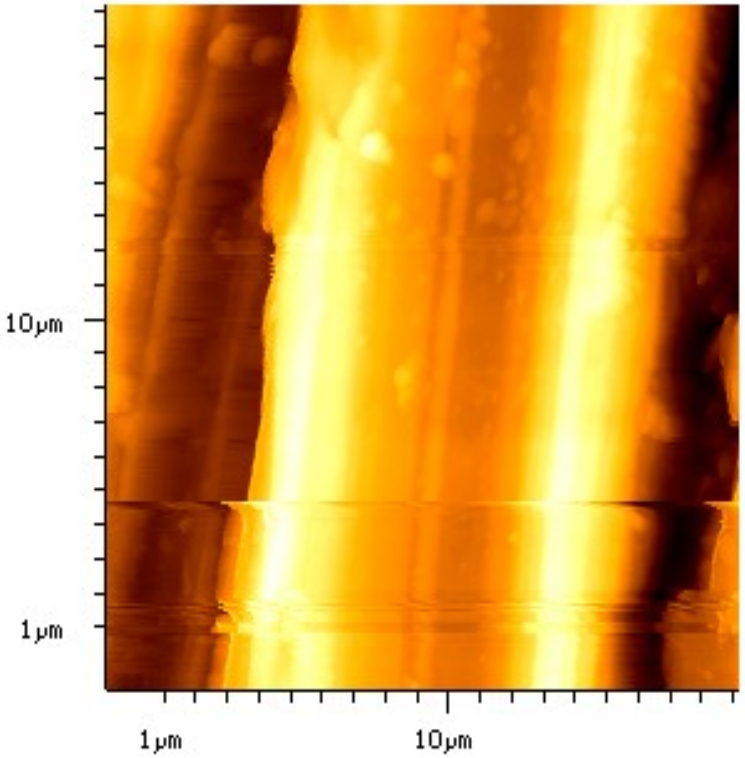

# Film characterization

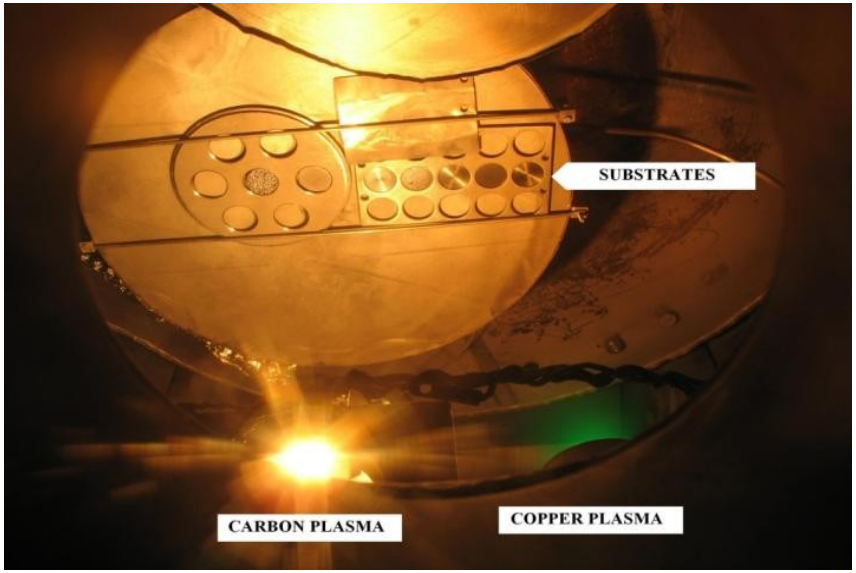


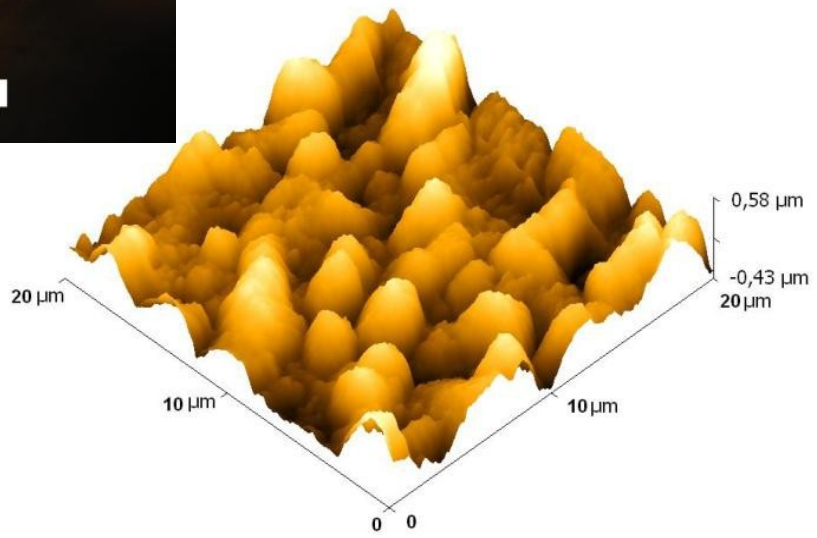

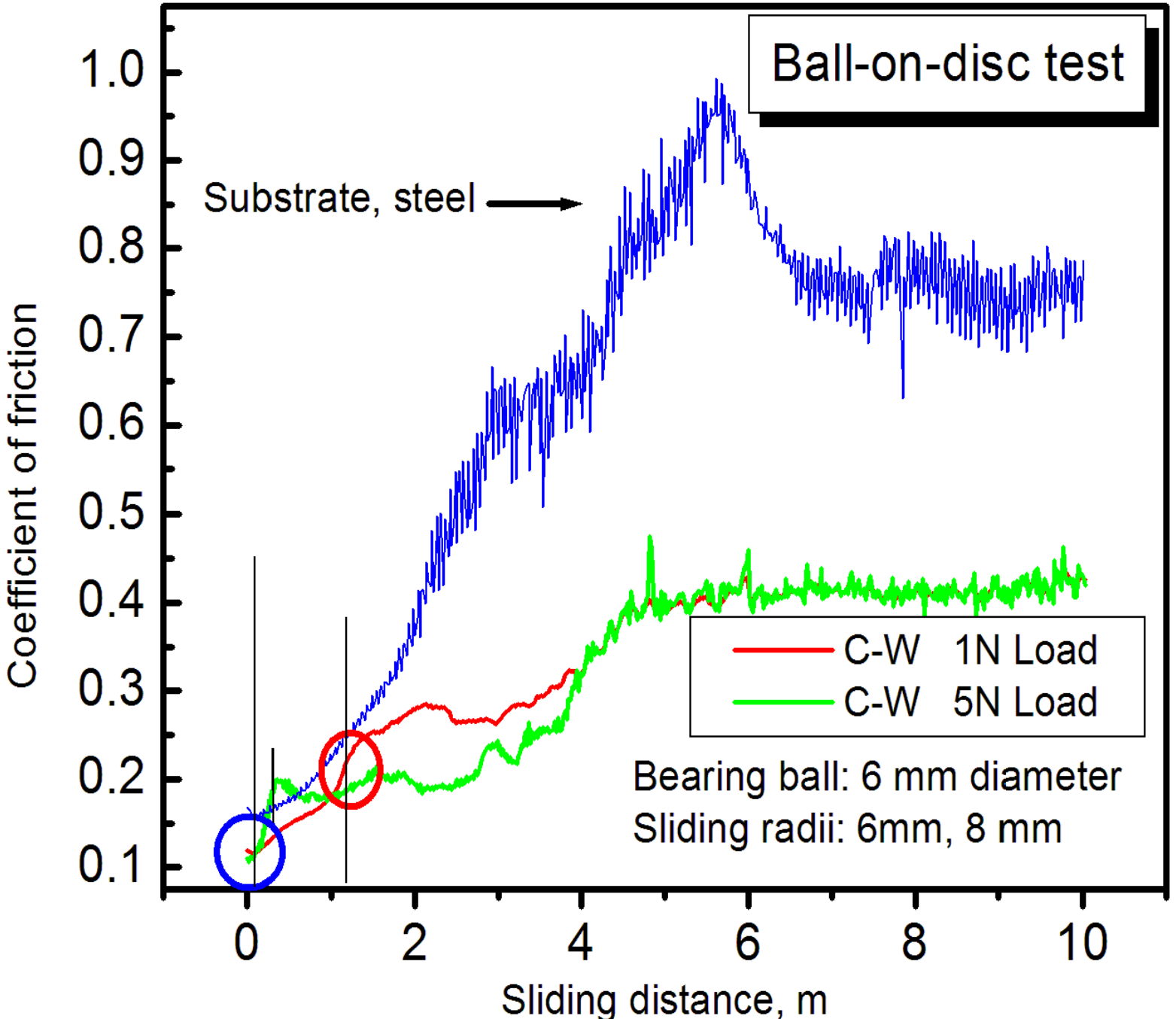
Ball-on-disc test
Substrate, steel
C-W 1N Load
C-W 5N Load
Bearing ball: 6 mm diameter
Sliding radii: 6mm, 8 mm
Coefficient of friction
Sliding distance, m
1.0
0.9
0.8
0.7
0.6
0.5
0.4
0.3
0.2
0.1
0
2
4
6
8
10

| Sample | Distance to W rod (mm) | Thickness (μm) | Hardness (GPa) | W (at%) | C (at%) |
|---|---|---|---|---|---|
| C-W 1 | 200 | 1.4 | 8 | 5.2 | 94.8 |
| C-W 2 | 220 | 1.6 | 11 | 9.5 | 89.5 |
| C-W 3 | 240 | 1.9 | 10 | 15 | 85 |
| C-W 4 | 260 | 2.0 | 14 | 20 | 80 |
| C-W 5 | 275 | 2.1 | 16 | 25 | 75 |

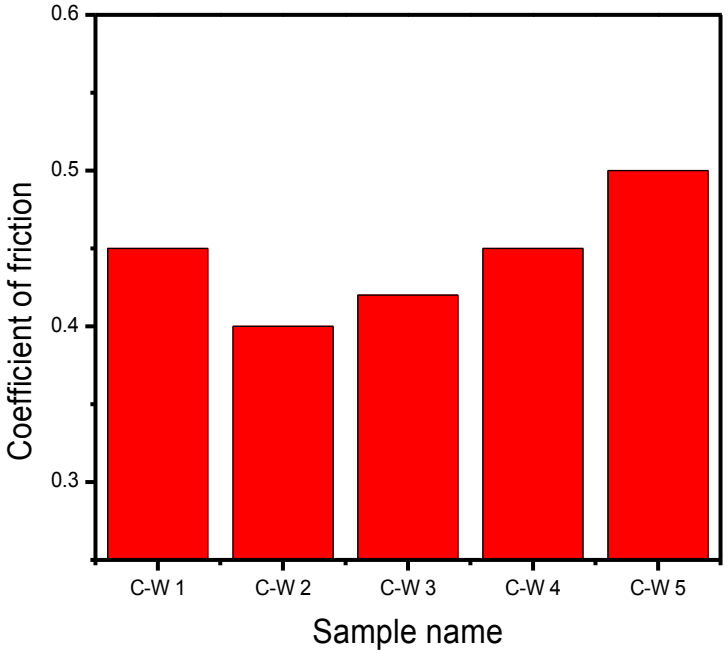

# (DLC) structure

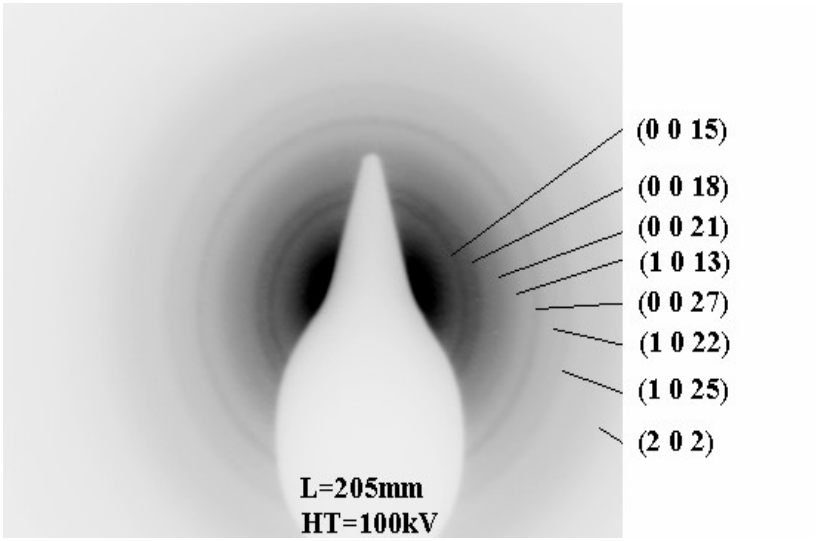


SAED

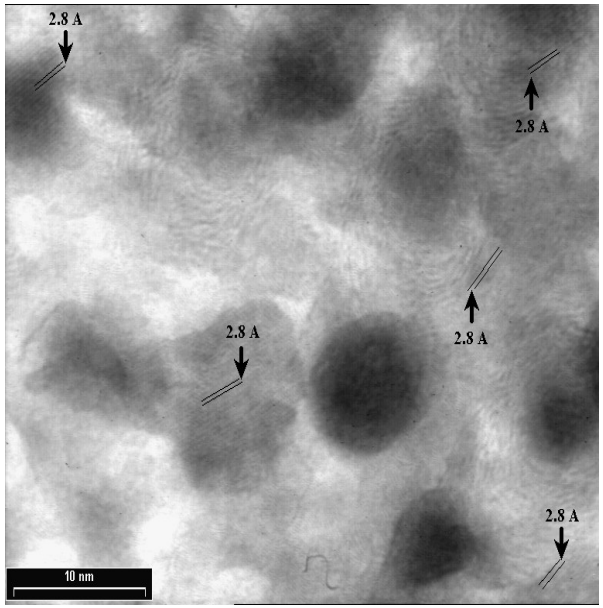


5nm HRTEM

Rhombohedra structures of the film with following parameters: a = 0.25221 nm, c = 4.3245nm (ASTM pattern: 79-1473) corresponding to diamond/carbon.

# Coefficient of friction C-Ni

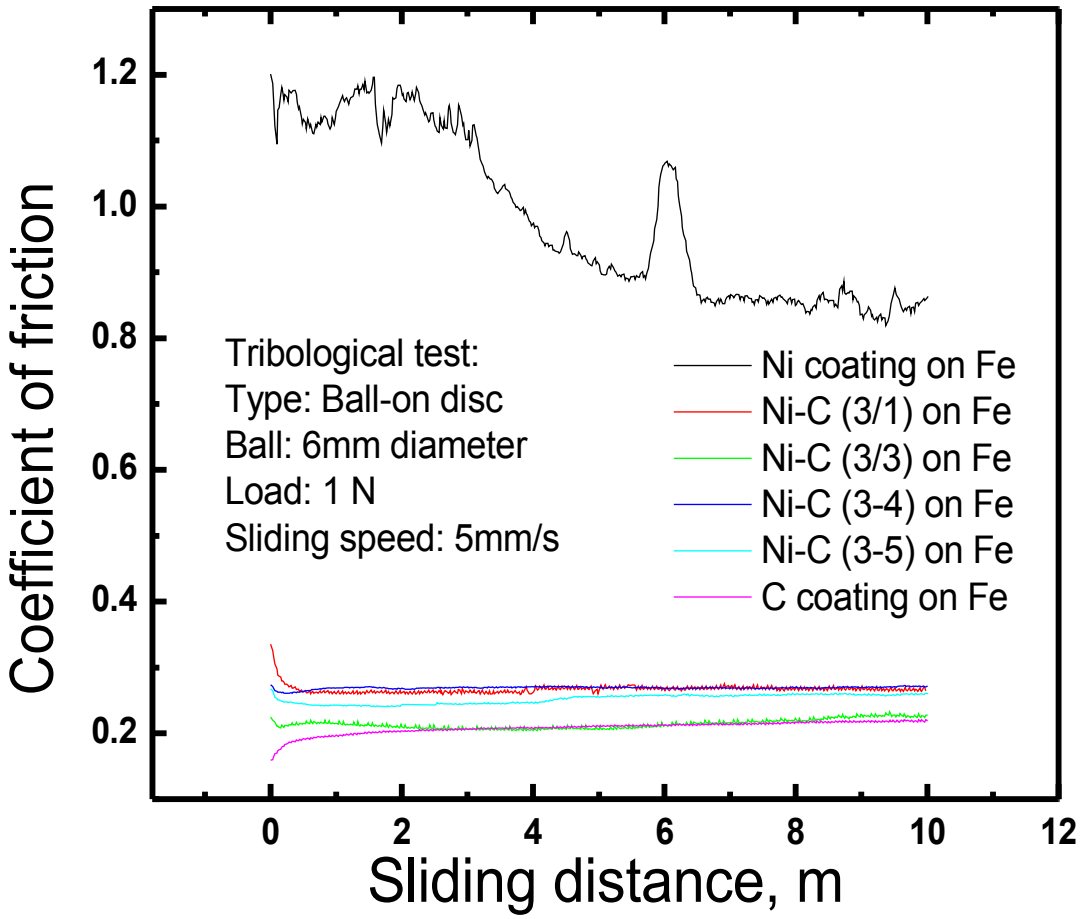

# Coefficient of friction C-Ni

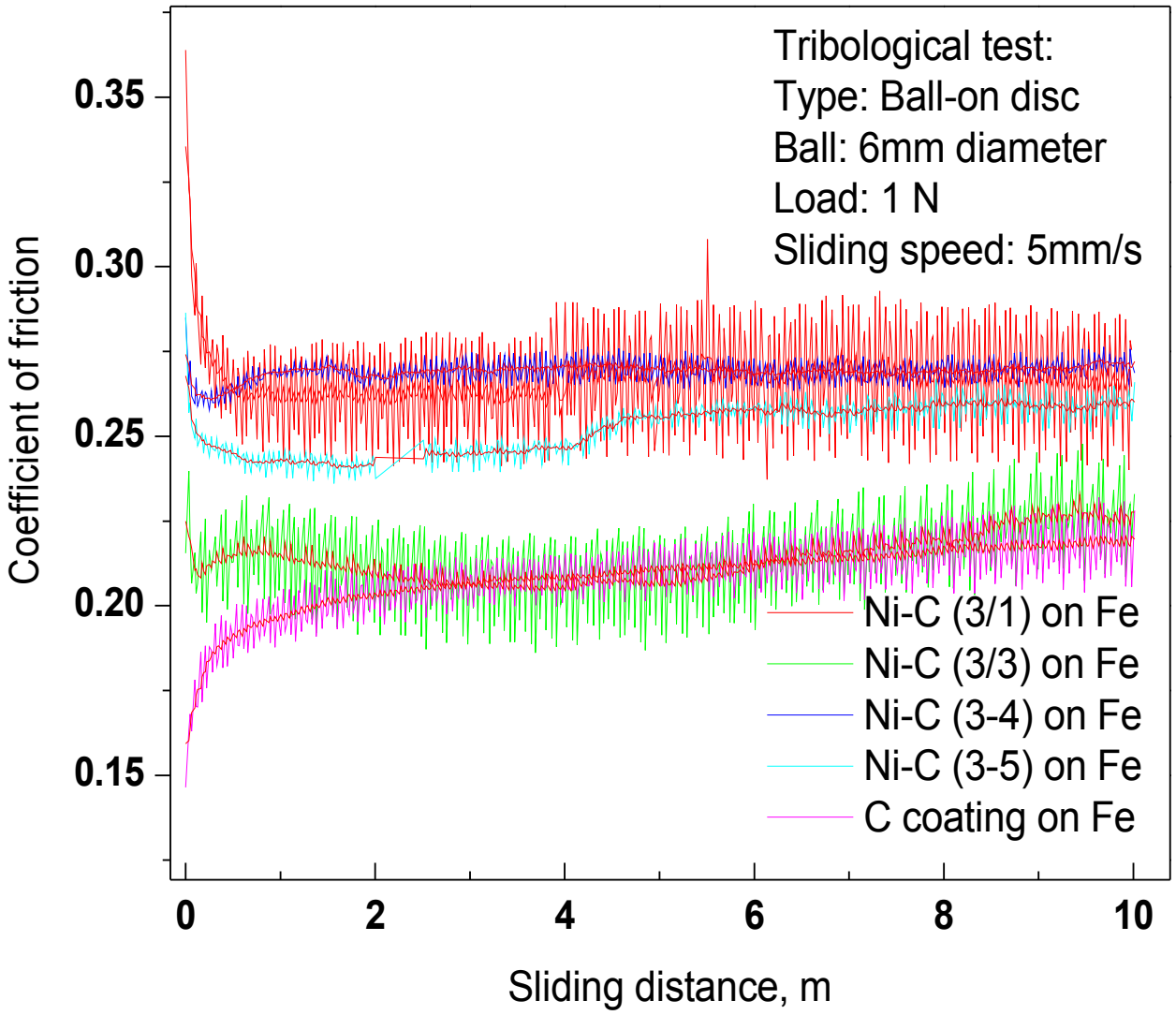

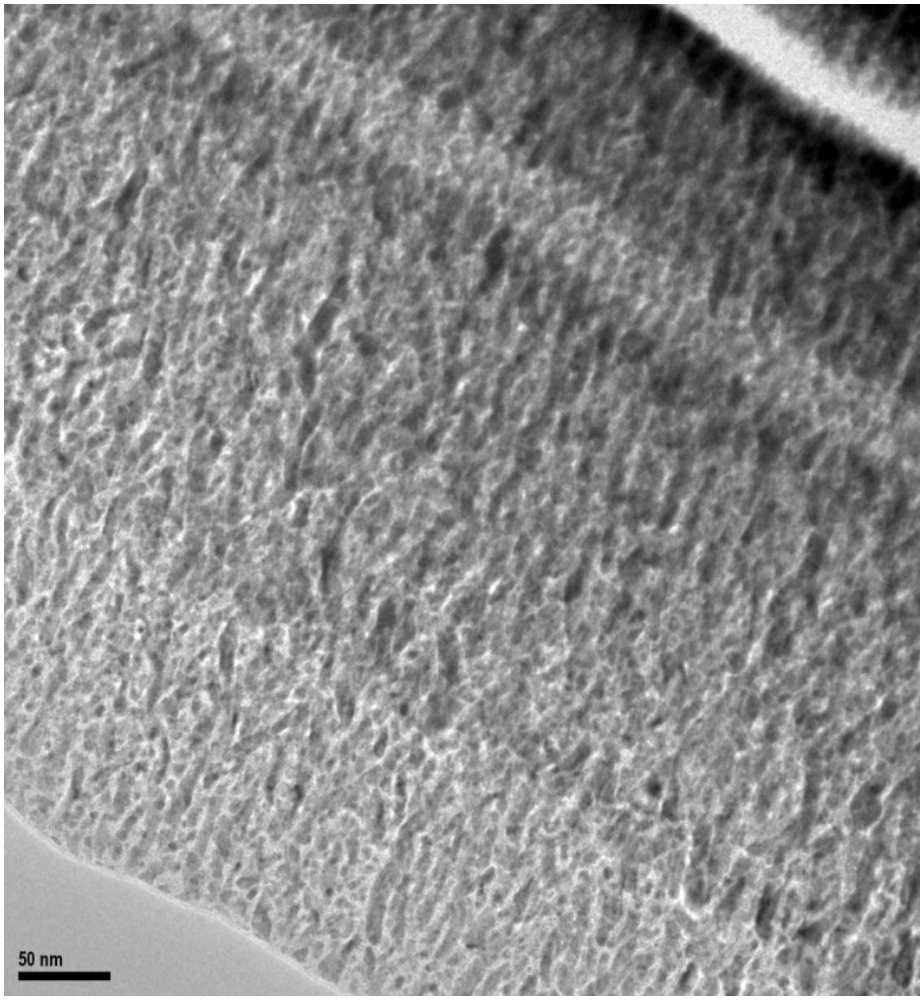


Images of the structure of the upper layer: tubular features with about 10 nm width and 50-100 nm length appear together with small grains with a lateral size of about 5 nm. The mentioned features are surrounded by a brighter matrix.

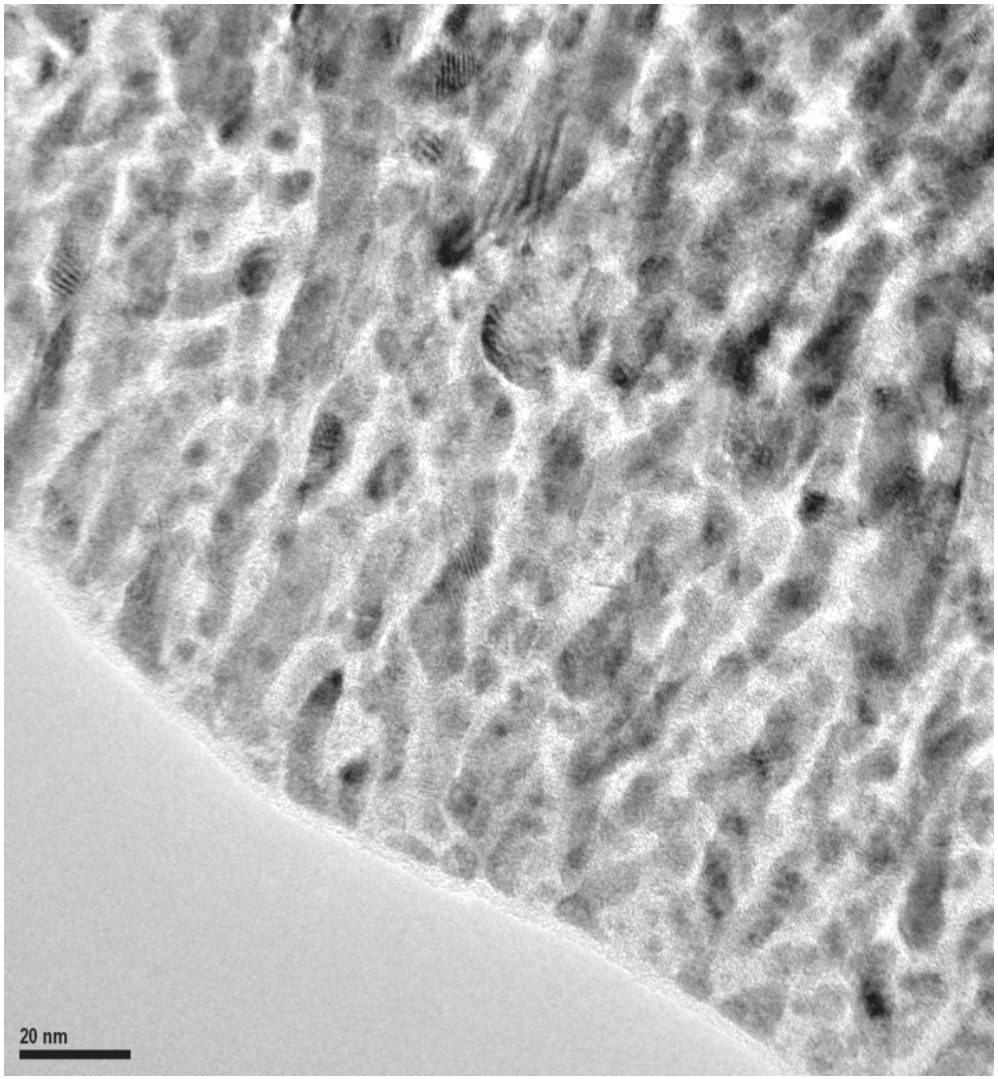


High resolution image of grains in the upper layer: in most of the grains a crystalline structure is visible, while the surrounding matrix is amorphous.

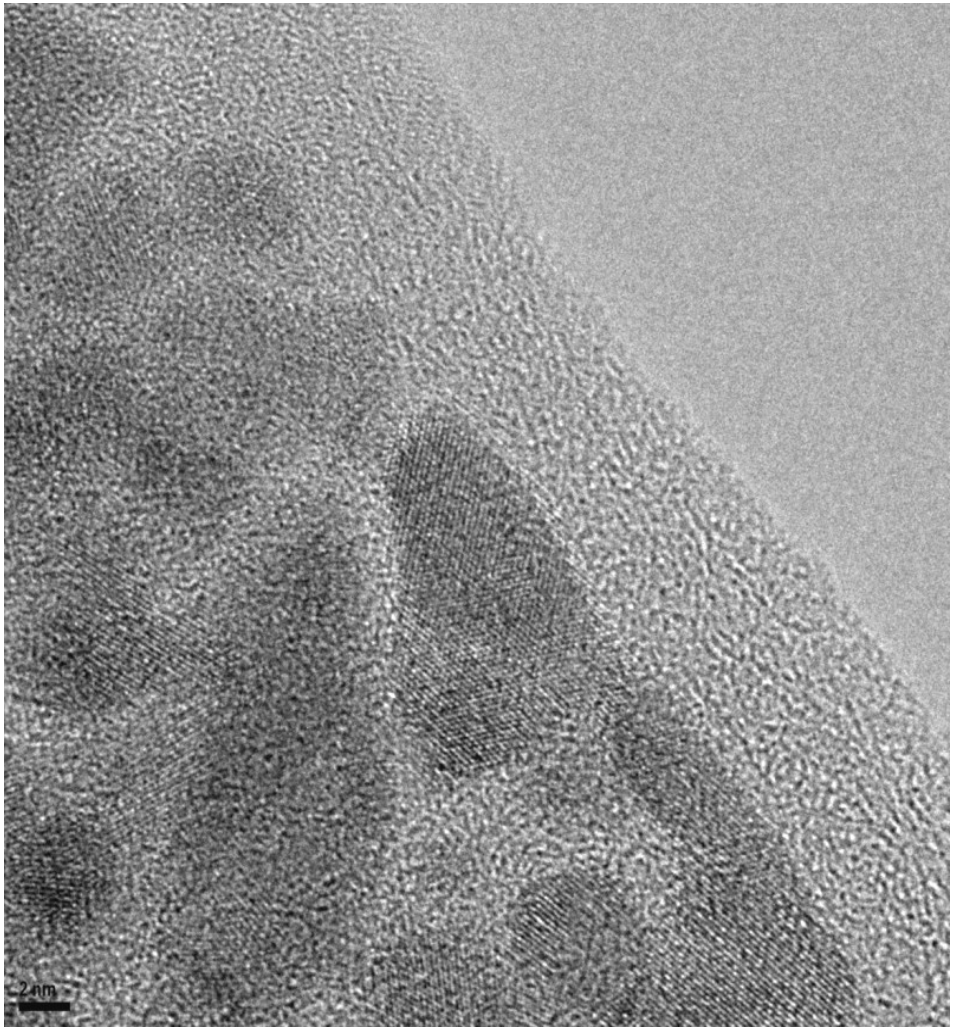


2 nm

High resolution image of grains in the upper layer: in most of the grains a crystalline structure is visible, while the surrounding matrix is amorphous.

# Acoperiri cu beriliu pe metale (Inconel si Nichel)

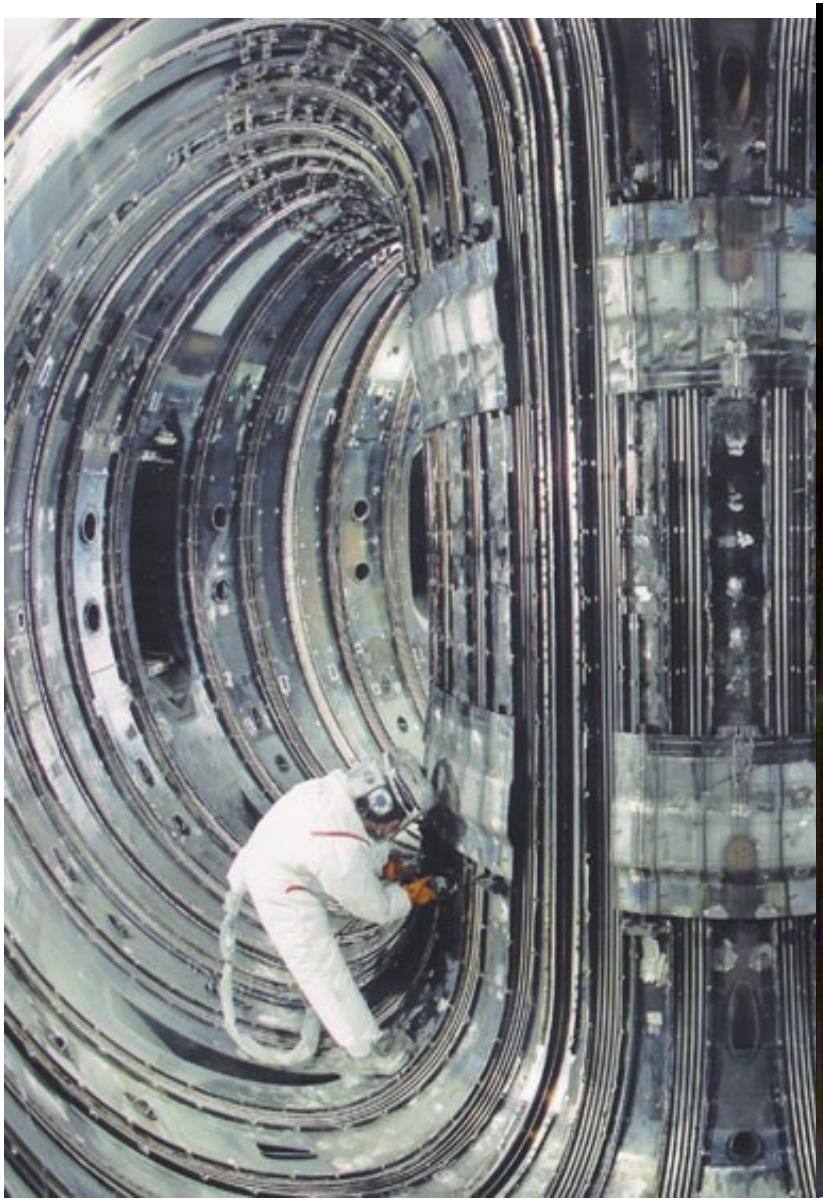

## Primul perete ITER & Materiale pentru Divertor

~ 700m$^2$ Be first wall :
low Z + Oxygen getter

~ 100m$^2$ W Baffle/Dome :
low erosion, long lifetime

~ 50 m$^2$ CFC Divertor Target
no melting, C good radiator

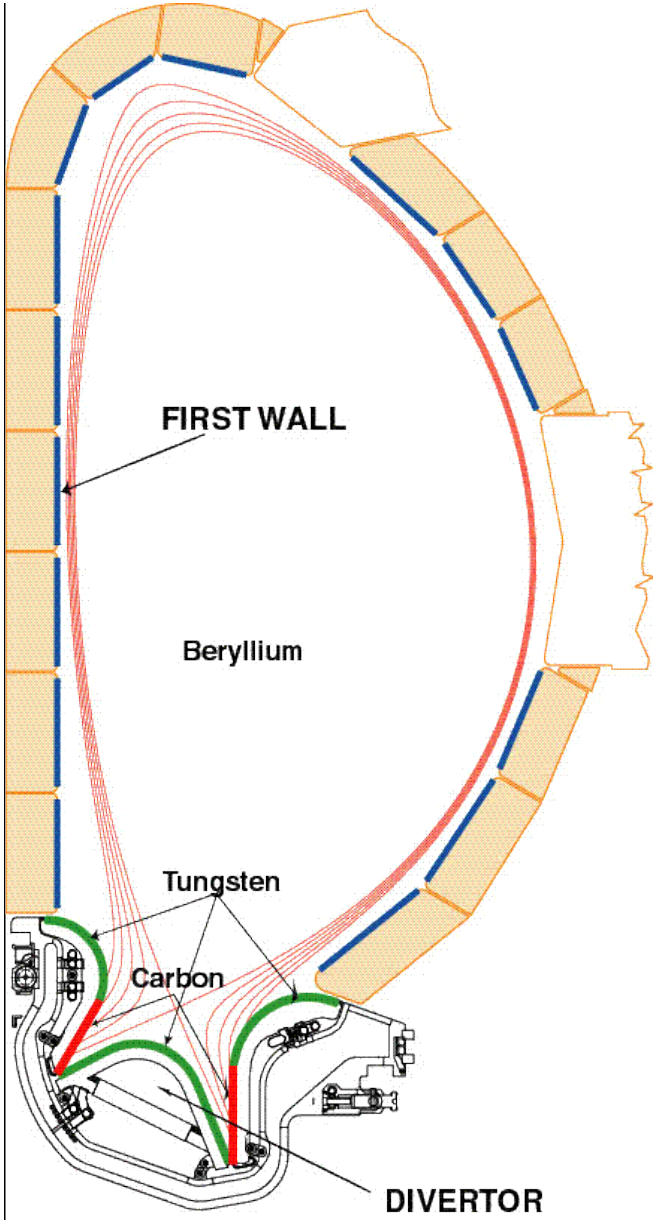

# Straturi marker din Be

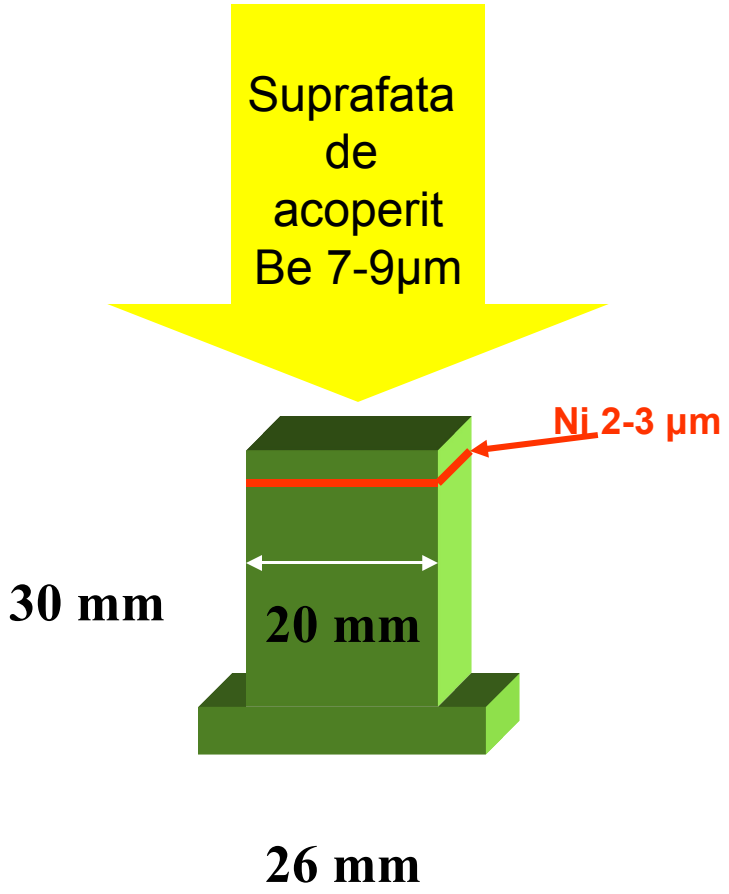


Heinzinger Power Supply

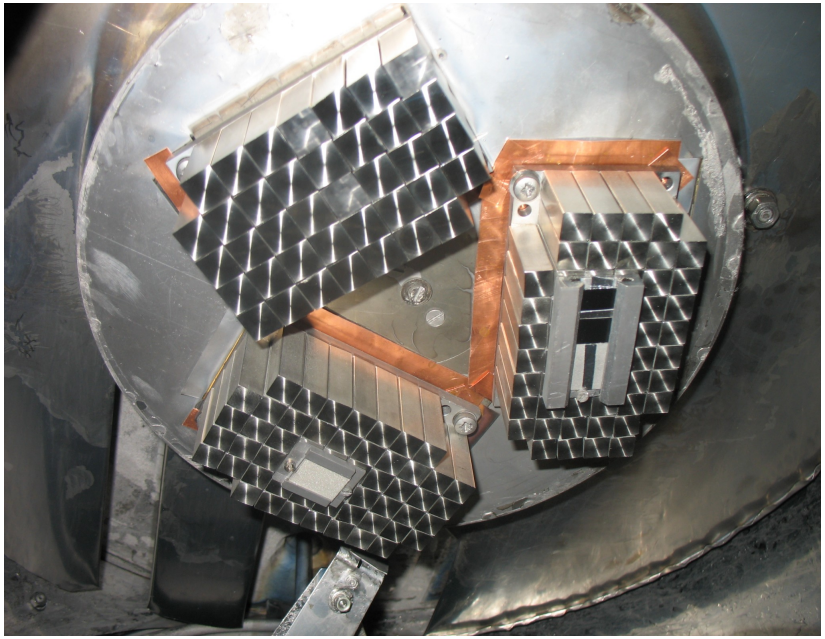

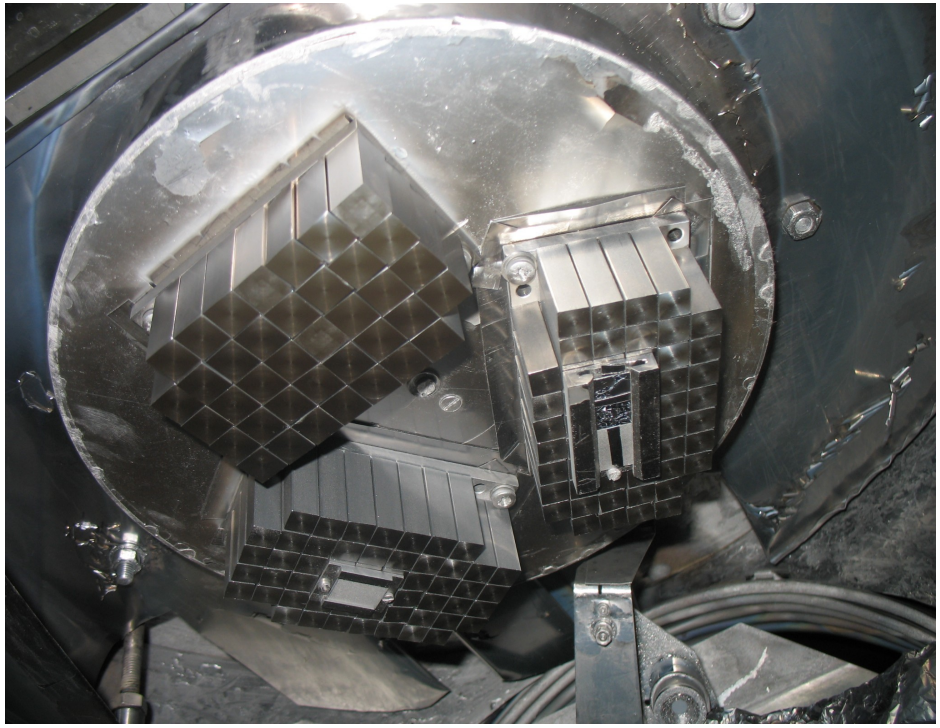

# Sectiune transversala in “caramizi inteligente”

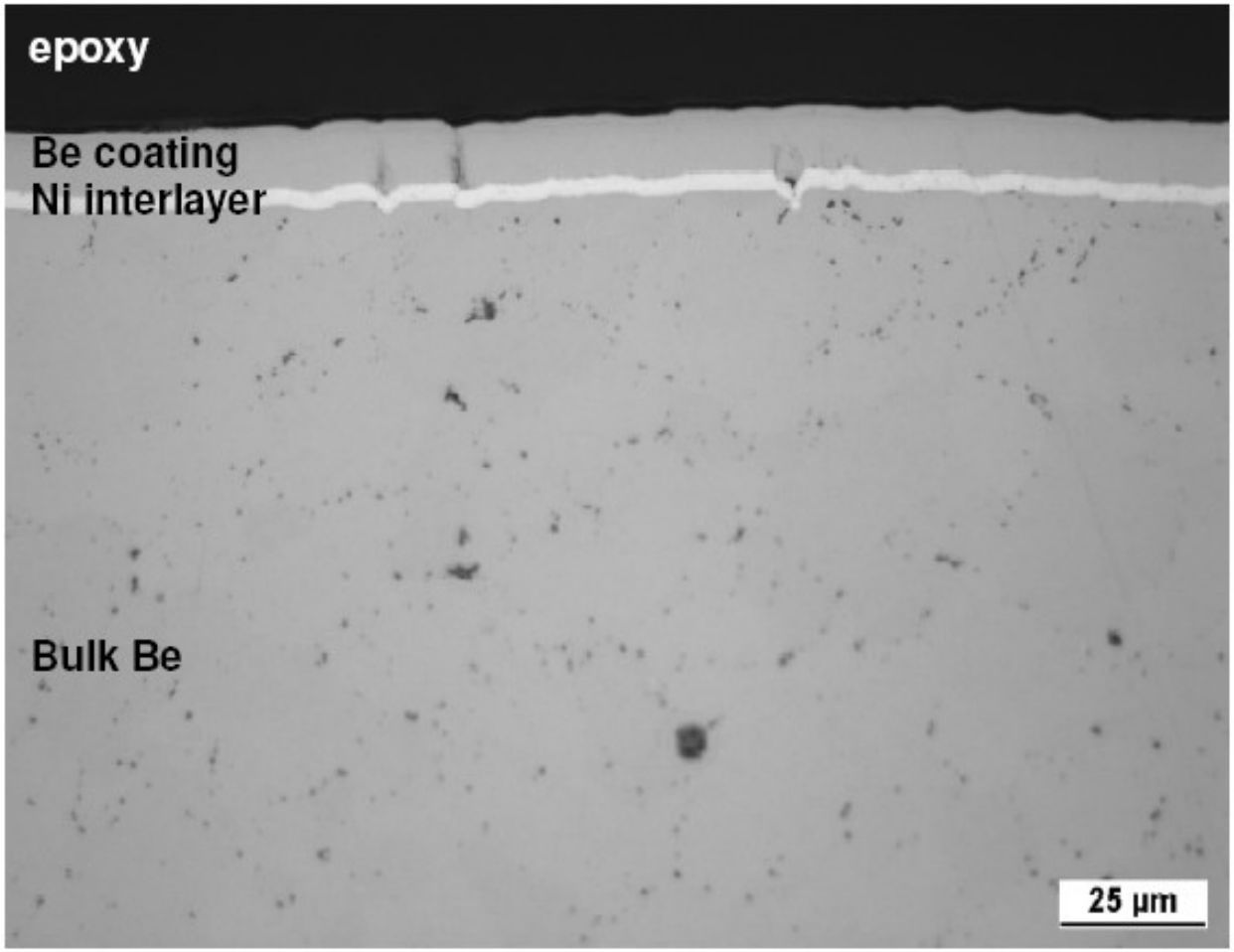


Fig. 16 TC28, 50 cycles of 3.5 MW/m$^2$ for 10s, optical image.

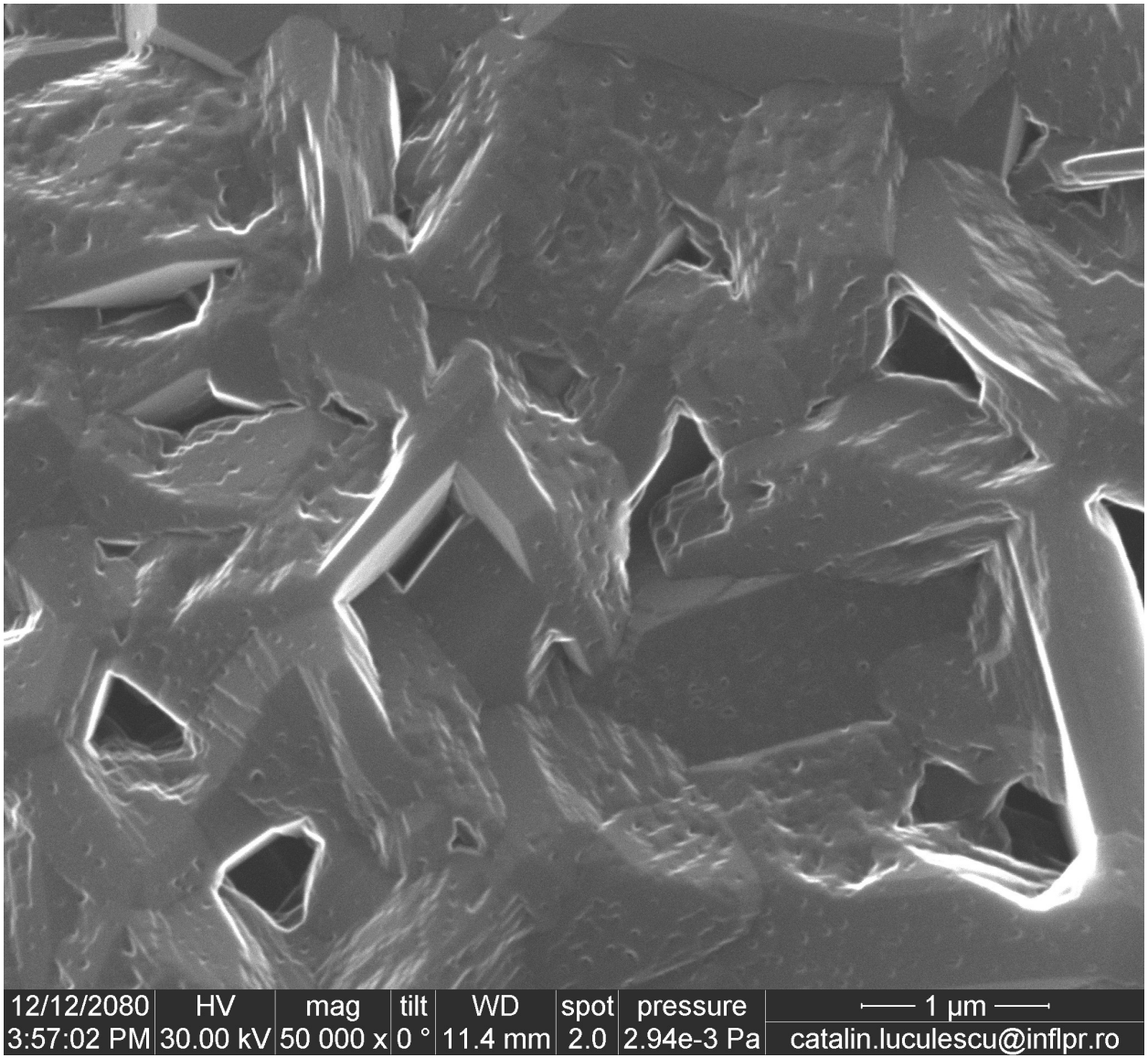
12/12/2080
3:57:02 PM
HV
30.00 kV
mag
50 000 x
tilt
0 °
WD
11.4 mm
spot
2.0
pressure
2.94e-3 Pa
1 µm
catalin.luculescu@inflpr.ro

Bias: +430 V

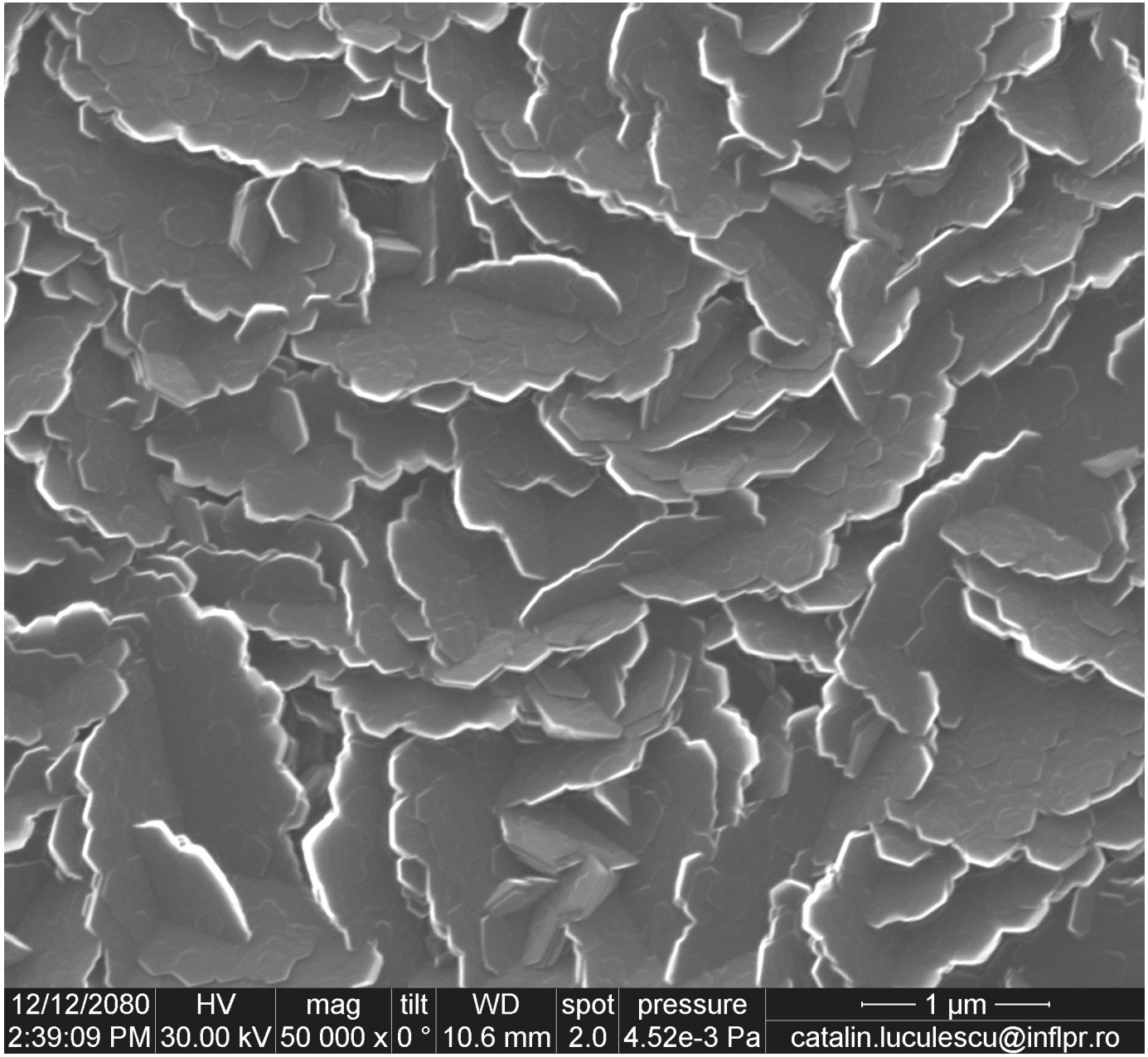
12/12/2080
2:39:09 PM
HV
30.00 kV
mag
50 000 x
tilt
0 °
WD
10.6 mm
spot
2.0
pressure
4.52e-3 Pa
1 µm
catalin.luculescu@inflpr.ro

Bias: 0 V

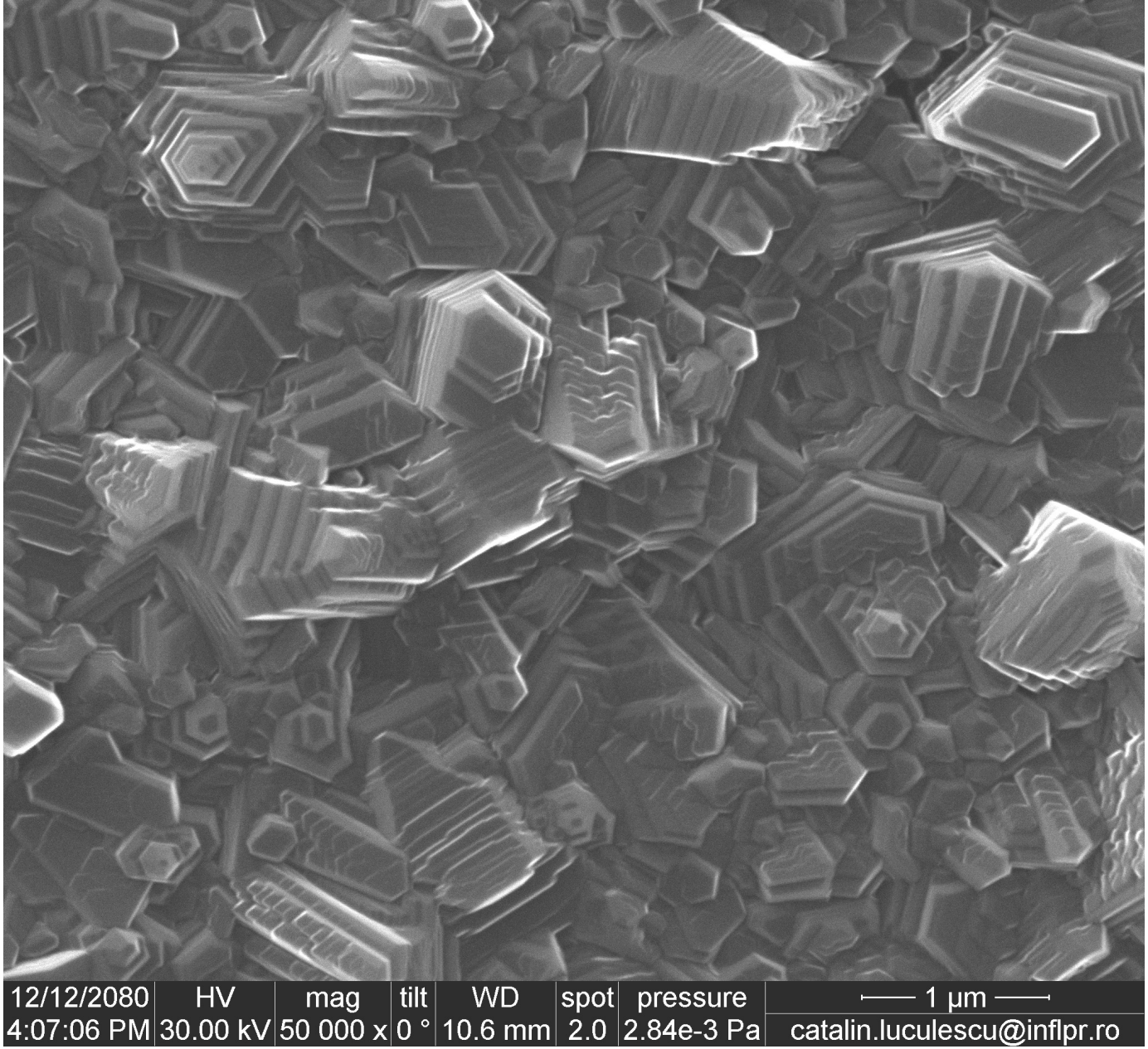
12/12/2080
4:07:06 PM
HV
30.00 kV
mag
50 000 x
tilt
0 °
WD
10.6 mm
spot
2.0
pressure
2.84e-3 Pa
1 µm
catalin.luculescu@inflpr.ro

Bias: -750 V

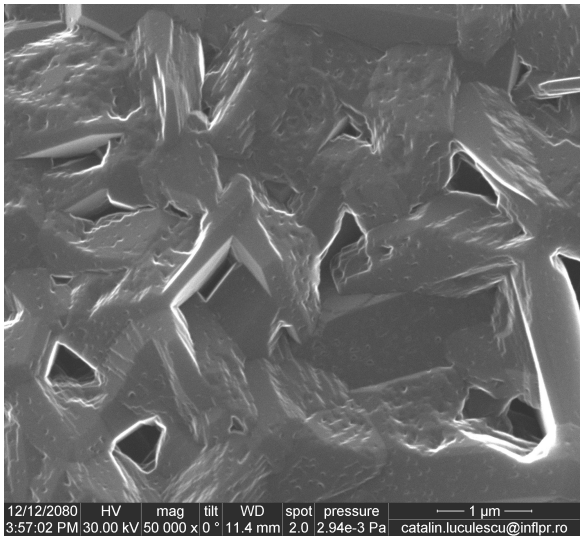


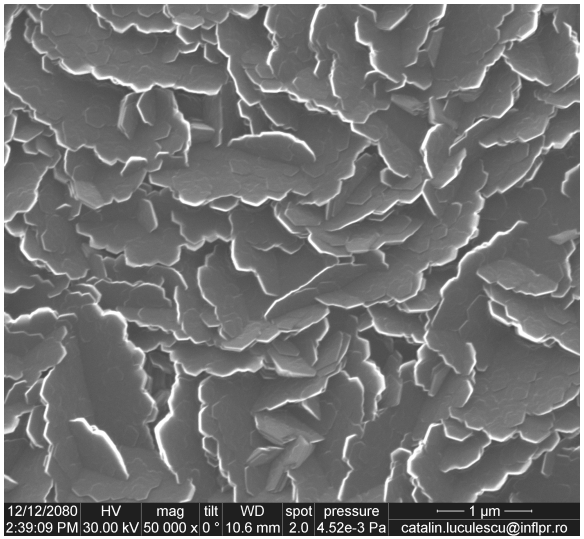


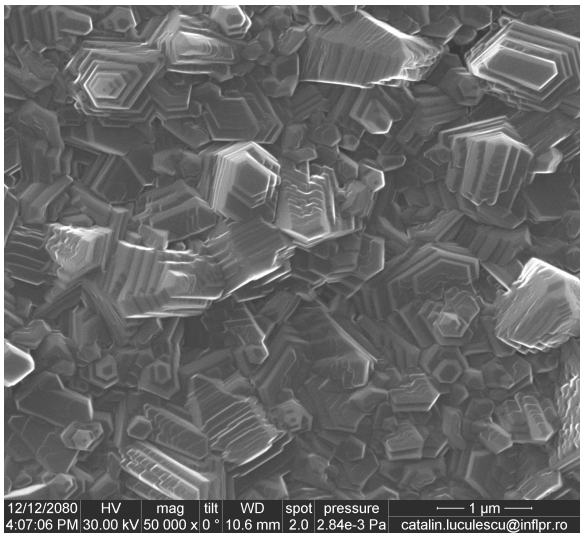


Bias: +430 V

0 V

-750 V

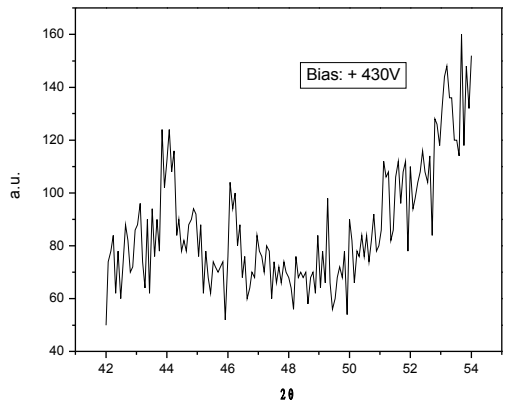


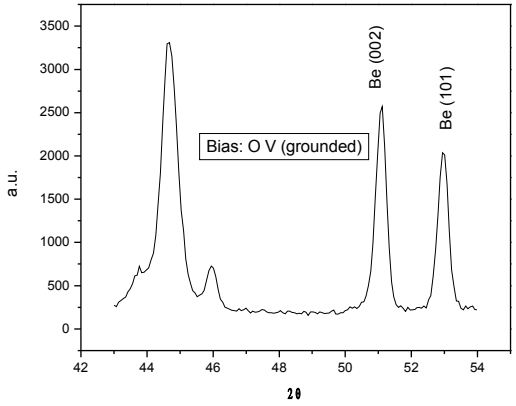


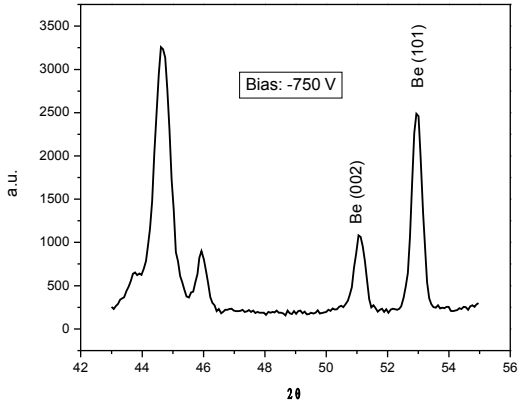

# Concluzii

**Folosind metoda TVA (arc termoionic in vid) s-au obtinut filme nanostructurate, functionale cu aplicatii in:**

- **Electronica (filme magnetorezistive)**
- **Mecanica (lubrifianti solizi)**
- **Tehnologii nucleare (filme compacte pentru acoperirea peretilor instalatiilor de fuziune)**